REPUBLIC OF TURKEY

ACIBADEM MEHMET ALİ AYDINLAR UNIVERSITY

INSTITUTE OF NATURAL AND APPLIED SCIENCES

DESIGN AND FABRICATION OF BIODEGRADABLE HYDROGELS AS ARTIFICIAL TISSUE SCAFFOLDS

Ali Murad ÖZMEN

MASTER THESIS

Supervisor

Assist. Prof. Özgül Gök

Co-Supervisor

Assist. Prof. Ceyhun Ekrem Kırımlı

ISTANBUL 2021

DECLARATION

I declare that this thesis has been composed by myself and it has not been submitted in any previous application for any other degree. Except for collaborative contributions, the experimental work and the data analysis were entirely done on my own. References have been used for supporting literature.

ACKNOWLEDGMENT

Firstly, I would first like to express my deep and sincere gratitude to my research supervisor, Assist. Prof. Özgül Gök for her patience, motivation, and enthusiasm. Her guidance has greatly helped me to perform this research and writing of this thesis.

I am grateful to my friends for always supporting me; Elif Gülin Ertuğral, İrem Soyhan, Gizem Canko,İleyna Sevde Üvak, Rabia Güner, Begüm Yalçın and Burçin Tatlıçeşme.

Finally, I must express my very profound gratitude to my parents (Rüçhan Cenk Kunter and Zeynep Kunter) and my partner Afife Karabayır for providing me with unfailing support and continuous encouragement throughout my education life.

This research has been supported by Acibadem Mehmet Ali Aydinlar University Scientific Research Commission (ABAPKO Project No: 2018/01/07 and ABAPKO Project No: 2019/04/03)

TABLE OF CONTENT

DECLARATION iii
ACKNOWLEDGMENT iv
LISTE OF FIGURES vii
LIST OF TABLES ix
LIST OF ABBREVIATIONS x
SUMMARY 1
ÖZET 2
1. BACKGROUND AND AIM OF THE STUDY 3
2. INTRODUCTION 5
2.1 Tissue Engineering 5
2.2 Cross-linking Strategies for Hydrogels 8
2.2.1 Nucleophilic reactions 8
2.2.2 Click reactions 9
2.2.3 Thiol-ene and thiol-yne chemistries 10
2.3 Hybrid Hydrogels as Reinforced Scaffolds 11
2.3.1 Synthetic polymer incorporation 12
2.3.2 Natural polymer incorporation 13
2.4 Peptide-Conjugated Hydrogels 15
2.5 3D BioPrinting of Scaffolds in TE 17
3. MATERIALS AND METHODS 19
3.1 Materials 19
3.2 Methods 20
3.2.1 Preparation of UV-curable hydrogels 21
3.2.2 Preparation of PLA incorporated hydrogels 22
3.2.3 Encapsulation of hyaluronic acid (HA) into hydrogels 23
3.2.4 Peptide immobilization into hydrogels 23
3.3 Characterization of Hydrogel Scaffolds 24
3.3.1 Gel conversion calculations 24
3.3.2 Rheological test of hydrogel scaffolds 24

3.3.3 FT-IR analysis of hydrogel scaffolds 25
3.3.4 Water uptake capacity determination 25
4. RESULTS 27
4.1 Preparation of UV-Curable Hydrogel Scaffolds 27
4.1.1 Preparation of TEGD-PE hydrogel 27
4.1.2 PLA incorporated hydrogel scaffolds 28
4.1.3 HA encapsulated hybrid hydrogel scaffolds 29
4.1.4 RGD immobilized (TEGD-PE-PLA+HA) hybrid hydrogels 30
4.2 Characterization of Prepared Hydrogel Scaffolds 31
4.2.1 Gel conversion determination 31
4.2.2 Water uptake capacity determination 33
4.2.3 FT-IR spectroscopy Analysis 35
4.2.4 Rheological analysis 37
4.2.5 Morphological analysis 39
4.3 3D Modelling and Printing 44
5. DISCUSSION 46
6. CONCLUSION 52
7. REFERENCES 54
8. APPENDICES 57
9. CURRICULUM VITAE 58

LISTE OF FIGURES

Figure 1.1. General Scheme for Biodegradable and Bioactive Hydrogel Scaffold Designed as Artificial Neural Tissue Piece..... 4
F**igure 2.1.** Thiol-ene (up) and Thiol-yne (down) chemistry mechanisms..... 10
Figure 2.2. Important Aspects in Scaffold Design..... 12
Figure 2.3. Advances in Crosslinking Strategies of Biomedical Hydrogel 15
Figure 2.4. 3D Bioprinting strategies for the preparation of tailor-made hydrogel scaffolds. 18
Figure 3.1. Chemical Composition of Bioactive and Biodegradable Hydrogel Scaffolds..... 20
Figure 3.2. Experimental Design for the Preparation of Hydrogel Scaffolds..... 21
Figure 3.3. Auto-Calculation Design for Gel Components..... 22
Figure 4.1. Water uptake capacity of UV crosslinked hydrogels..... 34
Figure 4.2. Water uptake capacity of PLA incorporated hydrogels..... 34
Figure 4.3. Water uptake capacity of HA encapsulated hydrogels 35
Figure 4.4. FT-IR spectroscopy analysis result for PLA incorporated hydrogels... 36
Figure 4.5. FT-IR spectroscopy analysis results of PLA incorporated &HA encapsulated hydrogels 36
Figure 4.6. Rheological assessments for PLA incorporated gels..... 38
Figure 4.7. Rheological assessments of PLA incorporated &HA encapsulated gels 38
Figure 4.8. Morphological analysis of PLA incorporated gels 40
Figure 4.9. Morphological analysis of PLA incorporated &HA encapsulated gels 41
Figure 4.10. EDS-SEM Analysis Result: Scan mode image of PLA incorporated &HA encapsulated peptide (RGD) immobilized hydrogel (H13) 42
Figure 4.11. EDS-SEM Analysis Result: Scan mode image of PLA incorporated &HA encapsulated peptide (IKVAV) immobilized hydrogel (H14)..... 43
Figure 4.12. 3D Printed PCL (poly-caprolactone) prototypes in different architectures with optimization purposes..... 45

Figure 4.13. Photo for 3D Printed bioactive hydrogel scaffold obtained in this thesis. 45
Figure 8.1. Raw Data for Rhelogical Analyses 57
Figure 8.2. Water Uptake Capacity (Raw Data) 57

LIST OF TABLES

Table 4.1. Composition details of TEGD-PE hydrogels 28
Table 4.2. Composition details of PLA incorporated hydrogels 29
Table 4.3. Composition details of HA encapsulated hybrid hydrogel scaffolds 30
Table 4.4. Composition details of RGD immobilized (TEGD-PE-PLA+HA) hybrid hydrogel scaffolds 31
Table 4.5. Calculated gel conversions of TEGD-PE hydrogel scaffolds 32
Table 4.6. Calculated gel conversion of PLA incorporated hydrogel scaffolds..... 32
Table 4.7. Calculated gel conversions of (TEGD-PE-PLA+HA) hybrid hydrogel scaffolds 33
Table 4.8. Calculated gel conversions of peptide immobilized (RGD or IKVAV) bioactive hydrogel scaffolds 33
Table 4.9. Element weight and atomic ratios obtained by SEM-EDS analysis for PLA incorporated & HA encapsulated hydrogel (H11) 41
Table 4.10. Element weight and atomic ratios obtained by SEM-EDS analysis for PLA incorporated & HA encapsulated peptide (RGD) immobilized hydrogel (H13) 42
Table 4.11. Element weight and atomic ratios obtained bySEM-EDS analysis for PLA incorporated & HA encapsulated peptide (IKVAV) immobilized hydrogel (H14) 43

LIST OF ABBREVIATIONS

0	Blank
CL	Cross-Linker
H	Hydrogel
HA	Hyaluronic Acid
Irg	Irgacure 2959
P10	%10 PLA (w/w)
PEP	Propargyl-ether PLA terminated
PLA	Poly (lactic acid)
TEGD	Tetra(ethylene glycol) dithiol

SUMMARY

Within the scope of this research project, the synthesis and characterization of bioactive hydrogels were accomplished. These hydrogels outstand as biomaterials with three-dimensional and porous scaffold structures. Integrated versions of various biomolecules to increase their application as a piece of artificial tissue in soft tissue engineering are of great interest for especially couple of decades not only in the literature but also in the market. In this project, three-dimensional hydrogel structures were obtained with a crosslinking strategy that has not been used in the literature before for this specific purpose. Thanks thiol-yne chemistry, it was possible to attach a short cell adhesion peptide covalently which contains a free thiol group in its structure and by this way, incorporates into this hydrogel scaffold to improve adhesion ability to live cells to polymeric walls.The thiol-yne reaction between the propargyl ether molecule, which has two alkyne groups in its structure, and the tetra (ethylene glycol) dithiol molecule with free thiol groups at both ends, was carried out by radical generation with the help of a photoinitiator and under UV light (365 nm). After the optimization steps, the hydrogel structure with the most suitable properties was selected and utilized for biomolecule (peptide) immobilization. Hyaluronic acid was encapsulated for enhancing mechanical properties to be more compatible with natural neural tissue features.

Keywords: Thiol-yne chemistry, Bioactive Scaffolds, Artificial Tissue Design, Interpenetrated Hydrogels, Hyaluronic Acid

ÖZET

Yapay Doku Iskelesi Olarak Kullanılabilecek Biyobozunur Hidrojel Skafoldların Tasarımı ve Geliştirilmesi

Bu araştırma projesi kapsamında biyoaktif hidrojellerin sentezi ve karakterizasyonu başarıyla gerçekleştirilmiştir. Bu hidrojeller, üç boyutlu ve gözenekli yapı iskeleleri olarak kullanılan biyomalzemelerdir. Yumuşak doku mühendisliğinde bir yapay doku parçası olarak uygulamalarını artırmak için hem literatürde hem de markette çeşitli biyomoleküllerin entegre edilmiş versiyonları özellikle son yıllarda büyük ilgi görmektedir. Bu projede, literatürde bu özel amaç için daha önce kullanılmayan bir çapraz bağlama stratejisi ile üç boyutlu hidrojel yapıları elde edilmiştir. Tiyol-yne klik kimyası olarak geçen bu yöntem sayesinde, serbest tiyol içeren ve bu hidrojel iskelesinin sağladığı polimerik yüzeylere hücre yapışmasını artırabilen bir peptit dizisinin yapıya kovalent olarak bağlanması mümkün olmuştur. Yapısında iki alkin grubu bulunan propargil eter molekülü ile her iki ucunda da serbest tiyol grupları bulunan tetra (etilen glikol) ditiyol molekülü arasında gerçekleştirilen bu reaksiyon, bir foto başlatıcı yardımıyla eadikal oluşturularak ve UV (365 nm).altında gerçekleştirilmiştir. Optimizasyon adımlarından sonra en uygun özelliklere sahip hidrojel yapısı seçilmiş ve biyomolekül immobilizasyonu için kullanılmıştır. Daha sonra, farklı oranlarda RGD ve IKVAV peptidleri içeren hidrojeller hazırlanmış ve SEM-EDS analizinde elde edilen hidrojelin tüm saflaştırma adımlarından sonra kimyasal yapısında peptid molekülleri taşıdığı tespit edilmiştir.

Anahtar sözcükler: Tiyol-in kimyasi, Biyoaktif Skafodlar, Yapay Doku Tasarımı, İç İçe Geçmiş Hidrojeller; Hyaluronik Asit

1. BACKGROUND AND AIM OF THE STUDY

This thesis aims to prepare three-dimensional tissue scaffold structures in the form of a hydrogel platform by using polymeric materials that have the potential to develop biodegradable and bioactive smooth network structures.

Within the scope of this project, it is achieved to prepare biodegradable and biocompatible hydrogel scaffolds that can act as artificial tissue. These hydrogel scaffolds were prepared by combining different synthetic and natural polymers and bioactive molecules like cell-adhesion peptides for controlling the physical-chemical properties of resultant scaffolds and to enhance both cell adhesion and proliferation. This hydrogel scaffold system seems to provide an opportunity to allow combining cell adhesion peptides and three-dimensional scaffold structures for both local applications of biomaterials and tissue regeneration in a controlled and directed manner. In addition, since no examples of this hydrogel scaffold combination have been found in the literature, this novel design can be evaluated as an advantageous artificial soft tissue platform with high potential in both improving wound healing and contributing to the regeneration of injured tissue at the applied damage site.

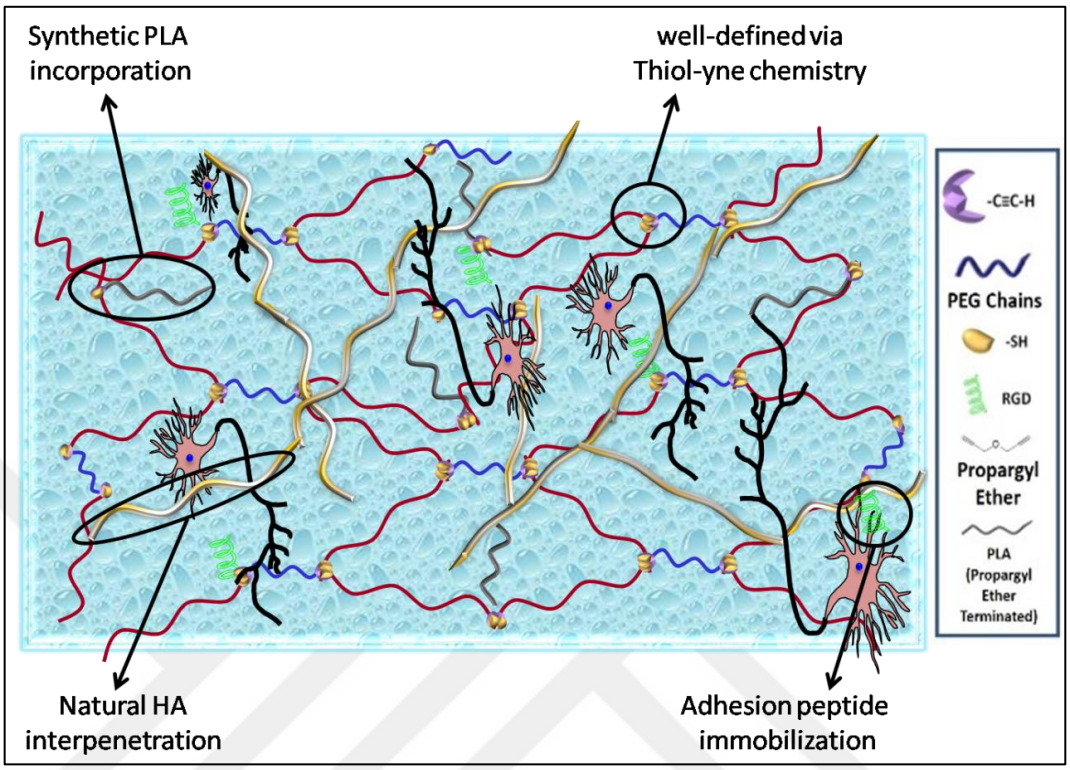

Figure 1.1. General Scheme for Biodegradable and Bioactive Hydrogel Scaffold Designed as Artificial Neural Tissue Piece

2. INTRODUCTION

2.1 Tissue Engineering

Patients with damaged organs have three options: transplantation, replacement, or repair, based on the situation and severity of the damage. Tissue technology, on the other hand, was seen as an effective way of saving lives and enhance the quality of life. Tissue engineering, which was first proposed in 1993, seeks to produce realistic replacements for injured tissue by combining biology and engineering concepts. Bioprinting is a renowned tissue engineering approach because it enables exquisite scaffold creation and cell distribution. Because of benefits such as precise deposition, cost-effectiveness, simplicity, and cell distribution controllability, 3D bioprinting development and application have been progressively growing in recent years. Most waiting lists for tissues and organs do not truly depict the magnitude of the crisis as only the sick seek such assistance (1).

Scientists and physicians commonly use the phrases regenerative medicine and tissue engineering interchangeably, thus they are used synonymously in this review. Regenerative medicine has demonstrated promising outcomes in the regeneration and replacement of a range of tissues and organs, including the skin, heart, kidney, and liver, as well as the ability to cure some chromosomal defects. Despite differences in national economic power, and thus differences in healthcare infrastructure, overcoming burdens such as shortages of organs and the practical challenges of collecting and storing them can help increase the number of people who can receive organ transplants. Bone morphogenetic proteins (BMP) for bone formation and platelet-derived growth factors for wound healing are instances of growth factors that have been used in this sense.

3D printing is one of the most remarkable technological advances in recent decades. Most importantly, biological material can be printed directly onto scaffolds which can then be seeded with cells. The majority of these scaffolds are constructed of ECM proteins along with synthetic polymers (2).

Synthetic scaffolds do not replicate the full range of properties found in native tissue and organs. Because body tissues and organs have both structure and function, any engineered material must be able of reconstructing the morphology and characteristics of the target tissue and organ. The application of life sciences and engineering to develop a basic understanding of the functional and structural relationships of natural and pathologic mammalian tissues, as well as the development of bio- substitutes that can be used to restore, maintain, or improve tissues damaged or lost by various disease conditions, was given as a comprehensive definition of TE.

To conclude, TE is the restoration, improvement, and maintenance of damaged tissues caused by a variety of factors such as disease, injury, or congenital disabilities (3). Currently, artificial scaffolds are used as a supporting structure for cell cultures and cell growth primacy in the repair of damaged tissues or organs. The scaffold's degradability eliminates the need to remove the material layer, and thus eliminates the side effects caused by foreign materials left in the body. The properties of the fabricated scaffold depend on the type of tissues that need to be repaired, whether they are hard tissues such as bones or soft tissues such as neural tissues. Cell regeneration involves the incorporation of cell differentiation (expanded or nonexpanded) extracted from a donor or a patient into a scaffold.

Hydrogels, for example, have been used to stimulate spinal cord tissue regeneration since they can adapt to the mechanical properties of spongy soft and viscoelastic neural tissue. Because of the rising demand for transplantation in clinical medicine, TE has become a feasible option. Scaffolds can function as cellular systems or as vehicles for cell and drug delivery in cell and tissue regeneration. An appropriate scaffold must be able to repair body tissues with minimal requirements, as well as enabling for cell development, vascularization, proliferation, and host integration, and materials must degrade naturally during or after the healing process. Tissue engineering, often known as regenerative medicine, is a multidisciplinary and interdisciplinary science that aims to develop viable biological substitutes that combine a scaffold, cells, and biological molecules to restore, preserve, or improve tissue function (4). Organic conductive polymers, due to their soft nature, have better mechanical compatibility and structural tun-ability with cells and organs than conventional electronic inorganic and metal materials. Polysaccharides and proteins are well-known natural polymeric biomaterials that have numerous applications in tissue regeneration.

Hydrogels are 3D crosslinked networks formed by polymers with hydrophilic properties. They are a type of novel smart biomaterial that responds to external stimuli and has potential applications as a scaffold for tissue regeneration and the delivery of bioactive molecules. A biomaterial scaffold is used in tissue engineering (TE) to provide mechanical and porous network structural support, shape, and hierarchy architecture, as well as surface chemistry for cell attachment, cell-cell communication through the porous network, proliferation, and differentiation for tissue regeneration. Biomaterial scaffolds are vital in any tissue regeneration because they not only provide temporary structural integrity but also play a role in cell-biomolecule interactions, cell attachment and growth, and tissue development. When surgical treatment is necessary, TE aims to develop new functional tissue and regenerate tissue in vitro or in vivo to cure illnesses. In these situations, 3D biomaterial scaffolds play a key role in damage repair.

A range of natural and synthetic polymers can be used to create 3D structured biomaterials. Tissue regeneration is introducing specific cell types or cell products to damaged tissues or organs to restore tissue and organ function. Mesenchymal stem cells, embryonic stem cells, and induced pluripotent stem cells are all stem cells that can be utilized for tissue regeneration. In response to certain ligands or growth factors, stem cells can differentiate into various cell types. The regenerative ability of stem cells was proven not only by growth factors but also by extracellular matrix proteins (5).

2.2 Cross-linking Strategies for Hydrogels

2.2.1 Nucleophilic reactions

While a variety of crosslinking chemistries has been devised to make cell-laden hydrogels for tissue engineering, thiol-based click reactions are becoming more relevant in the industry because they allow for the easy insertion of biological functions into synthetic hydrogels. A vast number of alternatives for generating precursor molecules and crosslinking them to generate hydrogels are accessible from a strictly chemical standpoint. However, the objective of encapsulating live cells imposes several particular criteria and constraints that must be taken into account (6). The first and most apparent need is that the crosslinking process is carried out in an aqueous and oxygen-rich environment. The selection of catalysts, initiators, and reactive functionalities is guided by this need, as well as the intended mode of gelation. The cytocompatibility of each component, on the other hand, must be thoroughly evaluated. Another worry is the hydrogel precursors' molecular weight, as lower molecular weight macromolecules might be taken up by cells and have a deleterious impact on viability. Low molecular weight poly(ethylene glycol) (PEG) acrylates, for example, are known to be cytotoxic, but their high molecular weight equivalents are not (7).

2.2.2 Click reactions

Lower molecular weights are harmful, while bigger molecular weights might be difficult for the body to absorb and excrete, which is critical for in vivo applications. The requirement for cell-compatible gelation conditions frequently entails the creation of semi-dilute solutions (e.g., mM), implying that the crosslinking reaction must happen quickly (ideally within 10 minutes), even when the functional group concentration is low. The wavelength of light used to commence photopolymerization is one of the most important parameters to consider. The shortest wavelengths of light that are appropriate for photopolymerization in the presence of cells are 350-365 nm, due to the well-documented damaging effects of ultraviolet (UV) radiation on cells, which can cause irreversible DNA damage (8). The commercial availability of very affordable light sources that irradiate a vast area and allow the production of several dozen samples in minutes makes 365 nm light very useful in the laboratory.

Photopolymerization using visible wavelengths (e.g., 405 and 530 nm) is becoming more appealing due to developments in light-emitting diode technology. Aside from wavelength, the dose is a crucial consideration, since extended exposure to high-intensity light can be harmful to cells. Exposures of less than or equal to 10 minutes at 10 mW cm^{-2} for 365 nm light are typically considered cytocompatible for this wavelength. The variety of photoinitiators is severely limited due to the wavelength and dosage requirements for cell encapsulation. 2-hydroxy-1-[4-(hydroxyethoxy)phenyl]-2-methyl-1-propanone, which is supplied commercially by Ciba under the product name I2959, is the most extensively employed UV photoinitiator documented in the biomaterials literature for cell encapsulation. Importantly, although being only marginally water-soluble (up to around 0.5 wt%, B25 mM), I2959 is cytocompatible at low doses (up to 0.05 wt%, B2.5 mM) and has been frequently used for photo-encapsulation of both primary cells and cell lines in hydrogels (9).

2.2.3 Thiol-ene and thiol-yne chemistries

Thiol-X reactions are promising for generating hydrogels via step-growth polymerization methods because of their quick reaction kinetics, specificity, and high yields. The main benefit of thiol-X chemistries for tissue engineering applications is that they make it easy to insert thiol-containing biological functions (such as cysteine-containing peptides or thiolated proteins) into synthetic hydrogels. When combined with synthetic PEG hydrogels, which interact with cells minimally due to PEG's hydrophilicity and lack of protein binding properties,thiol-X chemistries can be used to engineer cell-instructive matrices by incorporating biological signals that mimic key aspects of the extracellular matrix (ECM) in which cells live. Notably, peptide inclusion is simple using this method since cysteine residues are easily included during solid-phase peptide synthesis (SPPS) and no post-synthetic oligo sequence alteration is required. Protein thiolation is also common but it's important to be cautious when evaluating the impact of modification and reaction conditions on protein function (10).

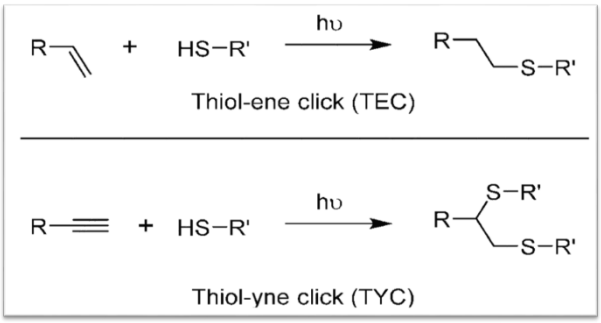

Figure 2.1. Thiol-ene (up) and Thiol-yne (down) chemistry mechanisms (27)

2.3 Hybrid Hydrogels as Reinforced Scaffolds

There are several different varieties of hydrogels, which may be categorized based on the materials used to make them, such as natural or synthetic hydrogels, or the processes used to make them, such as physical or chemical cross-linking. Chemical hydrogels (e.g., photopolymerized or enzymatically cross-linked) feature stronger stability and mechanical qualities (e.g. enhanced hydrogel stiffness). They are particularly useful for producing hydrogels with excellent biocompatibility, customizable viscoelasticity, and, most importantly, the capability to convey, protect, and release cargo to responsively surrounding tissue (e.g. triggered by biological substrates like glutathione for glutathione-mediated cleavage of maleimide-thiol adducts, or triggered by a change in pH) (11).

Chemically, functionally and morphologically distinct structural elements, such as biologically active proteins, peptides, or nano/microstructures, are interconnected by physical and chemical means in hybrid hydrogels. The heterogeneity of hybrid hydrogels can help improve cell adhesion, organization, and cell-cell interactions, resulting in tissue structures with improved mechanical integrity, electroactivity, and cellular organization. By allowing for the customization of micro-scale hydrogel properties (ideal for cell adhesion, migration, and proliferation) as well as the inclusion and customization of drug or gene delivery characteristics, hybrid hydrogels create new possibilities in biomedical applications (suitable for microenvironment-sensitive and targeted therapy) (12).

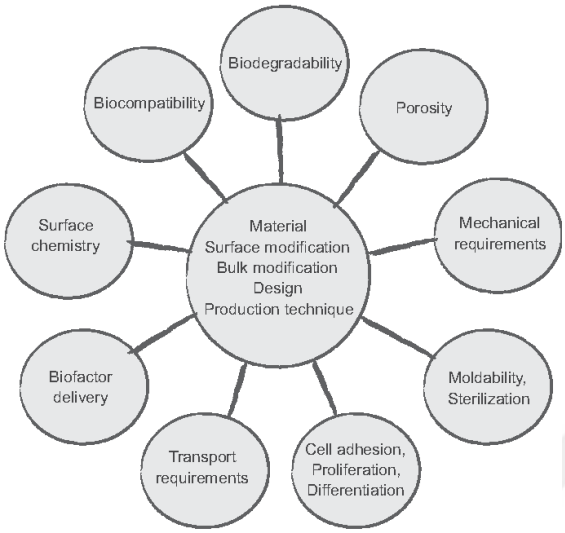

Figure 2.2. Important Aspects in Scaffold Design(28)

2.3.1 Synthetic polymer incorporation

Hydrogels in general have a range of characteristics that make them an intriguing study topic: they offer a high degree of versatility since their chemical and physical properties may be modified to create a gel that is best suited to the application. Hydrogels' unique capacity to create swelling 3D networks allows them to diffuse chemicals and cells, while their similarity to real soft tissue makes them appealing for medicinal uses as well (13).

The kind of monomer represented in the homopolymeric hydrogel, as well as the polymerization technique used in its synthesis, usually determine whether or not the hydrogel backbone structure will be cross-linked. Copolymeric hydrogels, on the other hand, are made up of two or more separate classes of monomers, with one of the two having hydrophilic qualities. On the backbone of the polymer network, this form of polymer arrangement has a polymer chain that is randomly distributed with a block or

irregular configuration. Synthetic hydrogels, on the other hand, are created from polyamides and polyethylene glycol, which are synthetic polymers. Natural hydrogels have been progressively replaced by synthetic ones or hybridized as stated above during the last two decades, resulting in increased service life, gel strength, and water absorption capacity (14).

2.3.2 Natural polymer incorporation

A direct strategy for bioactive hydrogel scaffolds for tissue engineering is created by combining the properties of synthetic and natural polymers to form hybrid hydrogels. By polymerization, cross-linking, and functionalization (modification by block structures, by blending, copolymerization), their molecular structure, molecular weight, chemical and physical properties (mechanical strength and biodegradability) are easily synthesized even at a large scale.

To address this limitation, protein-polymer hybrid networks with complicated capacities such as bioactivity, stimuli-responsiveness, catalytic activity, or the ability to regulate cell behaviors have been developed. Supramolecular hydrogels are created by combining particular peptide sequences (cell adhesive and/or enzymatically cleavable) to polymer chains to form blocks of peptides and polymers. Because the components may self-assemble into hybrid hydrogels either as peptide-polymer conjugates or by combining separate components, regulated cell responses (adhesion, migration, and differentiation) may be accomplished. Responsive hybrid hydrogels customized to a specific application can be developed by optimizing the amino acid sequence. The design and synthesis of hybrid peptide/polymer molecular hydrogels demonstrated significant research progress in simulating natural proteins' molecular architectures, dynamic

responsiveness, and cellular functions, while also providing tunability and processability provided by the synthetic polymer constituents (4).

Hybrid hydrogels were developed to address and alleviate these issues, as well as to expand the range of applications from medicinal (e.g. spatially and temporally controlled drug release profiles to optoelectronics and magnetic materials (e.g. high-tech applications such as fabrication of organic electronic devices with excellent charge transport and related properties.

Hydrogels with reversible or non-covalent cross-links, as well as hydrogels made up of supramolecular polymers or assemblies, have unique features for tissue engineering. The use of light to mediate changes results in a rapid response time, with micron-scale patterning possible in 3D using 2-photon irradiation. The technique employed to produce polymerization or cross-linking can have a massive effect on a hydrogel scaffold's characteristics and applicability. In this subsection, we will go over some of the most essential factors to consider while designing a hydrogel. The choice of initiator and activation wavelength, on the other hand, is vital. Many early reports relied on the UV-activation of poorly cytocompatible initiators as Igracure As a result, there has been a transition toward initiators with lower cytotoxicity that can be activated with less harmful visible light. Although the penetration of light through thick material and tissue limits the size of gels that may be formed, these approaches are increasingly being employed to initiate hydrogenation *in vivo* applications (11).

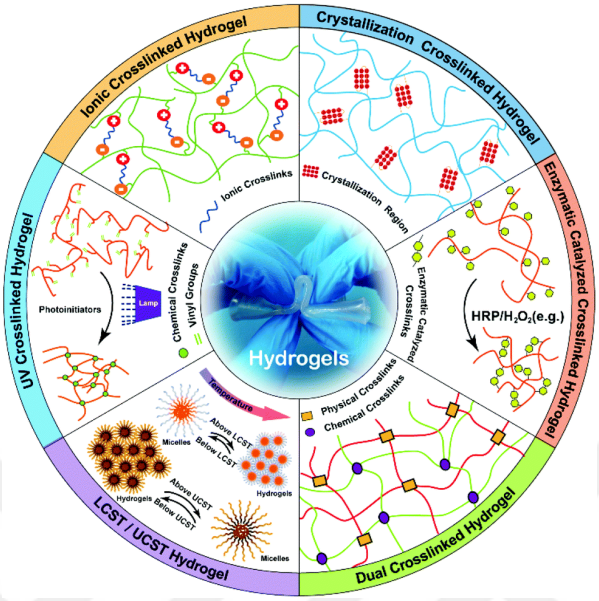

Figure 2.3. Advances in Crosslinking Strategies of Biomedical Hydrogel (29)

2.4 Peptide-Conjugated Hydrogels

The use of biomaterials with specific cell-adhesion ligands can potentially control the tissue formation or regeneration processes. However, for proper development of the tissue, there are critical steps need to understanding of interactions of cells with biomaterials and their impact on tissue formation. One of them is the production of extracellular matrix (ECM) components. The amount of ECM produced by the cells growing on a scaffold is critical for tissue formation due to its impact on the viability of the product. The potential use of nanomaterials in biomedical applications depends on their ability to integrate with cellular and physiological systems (15).

Several studies show *GRGDSP* and *IKVAV* peptides (The sequences correspond to Gly-Arg-Gly-Asp-Ser-Pro and Ile-Lys-Val-Ala-Val, respectively.) have been used to

coat materials surfaces. *GRGDSP* is a fibronectin-derived peptide with the ability to increase integrin-mediated cell adhesion via the cell-binding *RGD* residues which promote cell adhesion, neurite growth, and intervene in integrin regulation of neuronal gene expression mechanism. Moreover, *IKVAV* is used to stimulate neuronal growth and axon regeneration purposes due to its laminin residues. To the selective chemical ligation, a cysteine residue was added to the sequences of both C-terminal parts of maleimide MWNTs in water. These two peptides were prepared by using a solid-phase peptide synthesis technique. The coupling between the tubes and the peptides was observed by HPLC (16).

Surface coating with cell-adhesive molecules improves mechanical properties of cell-surface contact. Integrin, a transmembrane cell receptor that binds selectively to different proteins of the extracellular matrix, mediated cell adhesion. According to the literature, integrins have a critical role in mediating cell adhesion through cytoplasmic signaling pathways.

In 2005, Auernheimer and his colleagues used the tailormade cyclic RGD peptides to bind αv integrins with different affinities to switch the cell adhesion properties. Surface coating with photochemically regulated molecules is a promising approach to achieve cell-adhesive and cell-repulsive areas on the surface of materials and provides surfaces with specific photolithographically accessible patterns (17).

In another study in 2006, Gelain and his colleagues tested *RGD*-based sequences from fibronectin (*RGDS*), collagen VI (PRGDSGYRGDS), and laminin-derived motifs (*YIGSR, IKVAV, PDSGR*) to develop a 3D cell culture system with mouse adult neural stem cells (18).

These peptides are found in hippocampal mouse motifs and laminin-derived motifs known for promoters of neurite regeneration and sprouting with other peptides *in vivo*. Besides, self-assembling peptides were produced using the solid-phase synthesis method have been used for the studies of cell attachment and survival.

Although in the human body, almost all the cells are embedded in a 3-dimensional (3-D) microenvironment, almost all tissue cells have been studied in 2-D surroundings. In a living organism, cells are surrounded in a 3-D environment with the other cells and extracellular matrix components. The extracellular matrix is a complex network including proteins such as many types of collagens, laminin, and the other ECM proteins that regulate the functions of the cells and provide mechanical properties. This environment of cells allows attachment between the cells and the basal membrane (19).

2.5 3D BioPrinting of Scaffolds in TE

Three-dimensional printing offers a variety of potential as a construction method for tissue engineering scaffolds. The range of biomaterials that can be utilized in 3D printing limits the applicability of this technology in the field of regenerative medicine and tissue engineering. The human body has remarkable regeneration potential, but it is limited by factors such as tissue type and the necessity for growth hormones for differentiation and physical size (critical defect). Any injury to a tissue greater than this threshold size necessitates external assistance. TE or regenerative medicine are terms used to describe this method of aiding tissue regeneration (RM) (20).

Acellular scaffolds with biological components and cell-laden scaffolds for tissue-mimicking are the two types of structures 3D printed for TE and RM. Tissues consist of several cell types, an extracellular matrix (ECM), and a multitude of signaling chemicals. Three-dimensional (3D) printing, also known as additive manufacturing or fast prototyping, is used widely in tissue engineering applications to build scaffolds to heal or replace damaged tissues and organs (4).

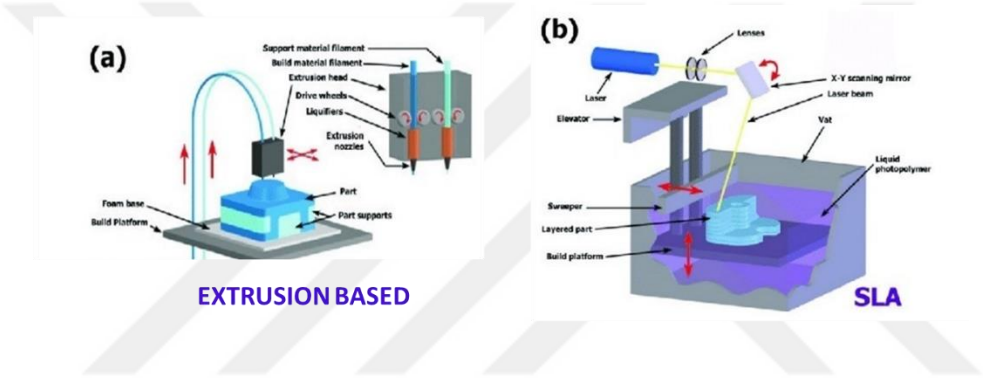

Figure 2.4. 3D Bioprinting strategies for the preparation of tailor-made hydrogel scaffolds. (21)

3. MATERIALS AND METHODS

3.1 Materials

Propargyl ether, 98%, Irgacure 2959, Poly(L-lactide) propargyl terminated average Mn 5000 Da, Tetra ethylene glycol, Hyaluronic acid sodium salt were bought from Sigma-Aldrich. N, N-Dimethylformamide (DMF) as peptide synthesis grade (for the synthesis of RGD and IKVAV) was bought from Acros Organics.

All chemicals in solid form (HA, RGD-C, PLA, Irgacure, and DMPA) were used as solutions prepared incompatible solvents for the gelation process. HA was dissolved in distilled water, meanwhile, RGD-C, PLA, Irgacure, and DMPA were dissolved in DMF according to the ratios revealed in the methodology section of this thesis.

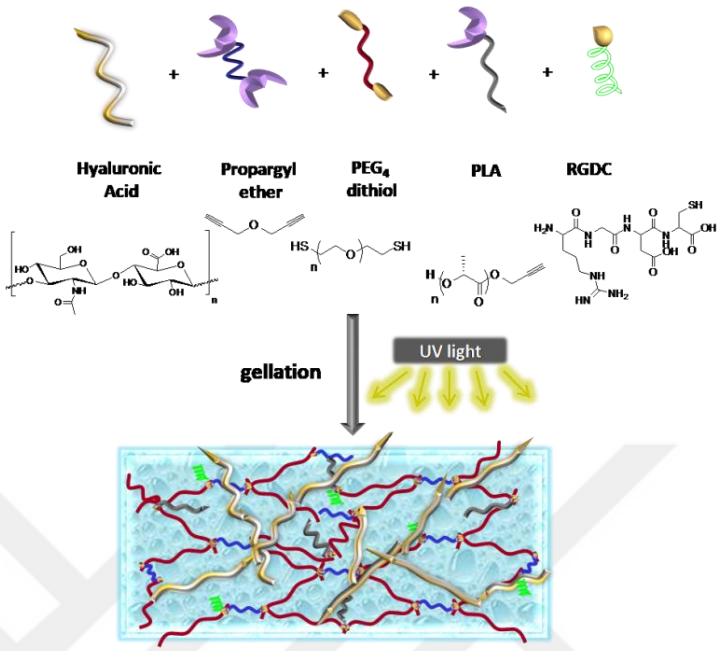

Figure 3.1. Chemical Composition of Bioactive and Biodegradable Hydrogel Scaffolds

3.2 Methods

Hydrogel scaffolds designed in this thesis were prepared as two successive platforms. First, PLA incorporated hydrogels were optimized and characterized widely. Then, their HA encapsulated and peptide conjugated versions were prepared. The procedures utilized for the synthesis of these hydrogels were modified based on the literature.

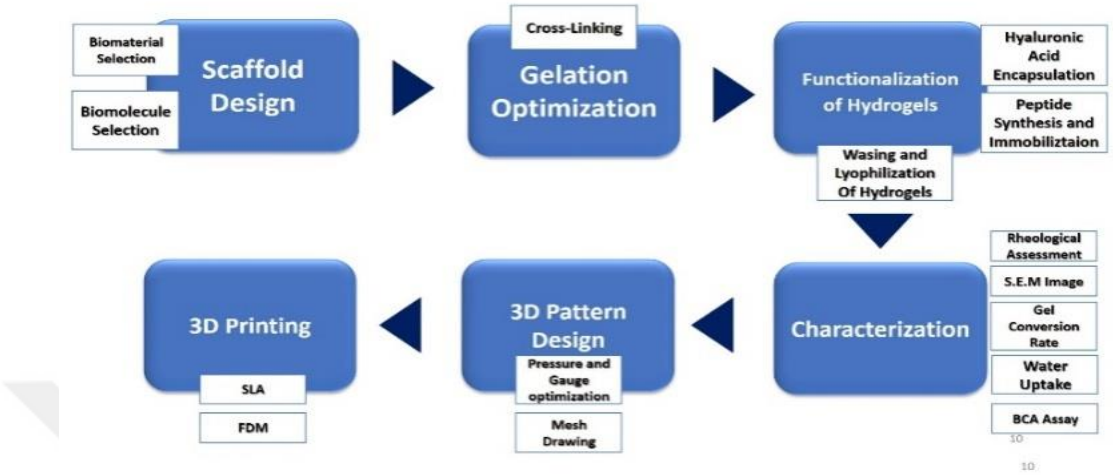

Figure 3.2. Experimental Design for the Preparation of Hydrogel Scaffolds

3.2.1 Preparation of UV-curable hydrogels

Two types of photo-crosslinkers (DMPA and Irg) have been used to prepare PLA incorporated hydrogels to observe the effect of photo-crosslinker type and UV exposure time. Briefly, 100 µL of TEGD and 25 µL PE were mixed under the hood at room temperature. Either 2.8 mg of DMPA or 2.4 mg of Irg was weighted separately and dissolved in DMF with a 1:4 ratio. All the chemicals were mixed thoroughly and DMF was then added to adjust the overall solvent ratio of the gel to 1:4. The prepared gel solutions were subjected to UV light via either a strong (UVP BLAK-RAY, B100VP) or weak UV source (UVP, UVGL-58) for different time intervals.

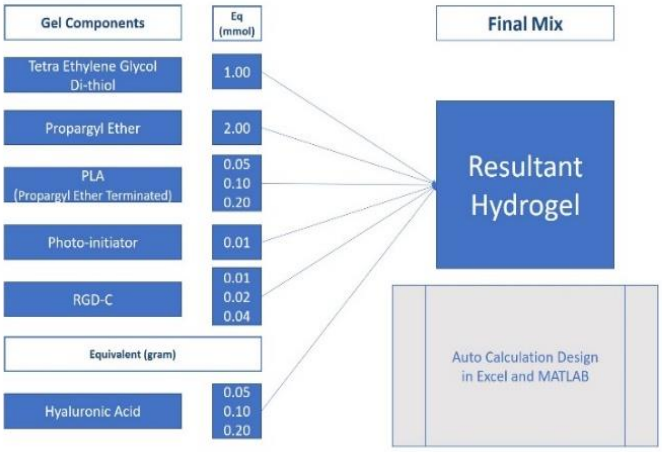

Figure 3.3. Auto-Calculation Design for Gel Components

3.2.2 Preparation of PLA incorporated hydrogels

Briefly, 100 µL of TEGD and 24.5 µL PE were mixed under the hood at room temperature. 25, 50, and 100 mg of PLA polymer were weighted (5, 10, and 20% w/w) dissolved in DMF with a ratio of 1:3. PLA solution (in DMF) was added to the mixture and stirred for 5 minutes under the hood. 2.4 mg of photocrosslinking was weighted to create a stock solutiıon with a ratio of 1:4, and 9.6 µL was added to the mixture. The mixture was placed under 365 nm UV for 1 hour for gelation. The obtained hydrogel was washed three times and prepared for characterization.

3.2.3 Encapsulation of hyaluronic acid (HA) into hydrogels

Briefly, 100 μL of TEGD and 25 μL PE were mixed under the hood at room temperature. 50 mg of PLA was weighted and dissolved in DMF with a ratio of 1:3. PLA solution (in DMF) was added to the mixture and stirred for 5 minutes under the hood. 2.4 mg of photocrosslinking was weighted to obtain a stock solution with a ratio of 1:4 and 9.6μL was added to the mixture. 20, 42, and 95 mg HA (5, 10, and 20% w/w, respectively) were weighed and dissolved in 100 μL water and added to the prepared gel mixture. The water DMF ratio was balanced in a constant ratio of 1:3 for all the gels. The final solute-solvent ratio was kept constant at a 1:4 ratio. The mixture was placed under 365 nm UV for 1 hour for gelation. The obtained hydrogel was washed three times with distilled water and stored at -20 °C for characterization studies.

3.2.4 Peptide immobilization into hydrogels

Briefly, 100 μL of TEGD and 25 μL PE were mixed under the hood at room temperature. 25, 50, and 100 mg of PLA were weighted (5, 10, and 20% w/w) dissolved in DMF with a ratio of 1:3. PLA solution (in DMF) was added to the mixture and stirred for 5 minutes under the hood. 2.4 mg of photocrosslinking was weighted to create a stock solution with a ratio of 1:4 and 9.6 μL was added to the mixture. 42 mg HA was weighted (10% w/w) and dissolved in 100 μL water and added to the prepared gel mixture. The water DMF ratio was balanced at a constant ratio of 1:3 for all the gels. The final solute-solvent ratio was kept constant at a 1:4 ratio. 6.93 mg RGDC was dissolved in DMF and added to the solution. The mixture was placed under 365 nm UV light for 1 hour for gelation. The obtained hydrogel was washed three times with distilled water and stored at -20 °C for characterization studies.

3.3 Characterization of Hydrogel Scaffolds

3.3.1 Gel conversion calculations

For this determination, before starting the experiment, the small glass bottles in which gelation would take place were tared. Afterward, the amount of material used was calculated in milligrams. As a result of gelation, small glass bottles are weighed, the amount of material used and the gel conversion was found by using tare.

Gel Conv. Rate = (weight of obtained H / feed weight of H components) x100 (eq. 1)

3.3.2 Rheological test of hydrogel scaffolds

Rheological characteristics of polymeric materials are tested at rheology research laboratories. Polymers, liquids, adhesives, and other samples are rheologically characterized under a variety of shear and extensional circumstances. Rheology characteristics are determined rheology labs for degradation research, molding parameters, material performance, and other applications. Understanding a polymer's rheological (flow) characteristics aids in obtaining optimal material properties throughout the molding process.

Rheology testing may tell you if your materials are being treated correctly and if there is little product deterioration. From single-point testing to variable shear-rate tests, rheological tests are used to determine the viscosity of polymeric hydrogels.

A wide range of shear, tensile, and extensional conditions can be used to characterize rheological properties. This information may be utilized for a variety of objectives, including quality control, product development, and gaining a better understanding of material performance. Rheology testing may also be used to verify if materials are correctly treated with minimum product degradation or to better understand flow properties.

3.3.3 FT-IR analysis of hydrogel scaffolds

The FTIR instrument transmits infrared radiation in the range of 10,000 to 100 cm^{-1} through a material, with part of it absorbed and some of it passing through. The sample molecules transform the absorbed light into rotational and/or vibratory energy. The resultant signal appears as a spectrum at the detector, generally ranging from 4000 cm^{-1} to 400 cm^{-1}, and represents the molecular fingerprint of analyzed samples.

3.3.4 Water uptake capacity determination

Hydrogels taken from +4 °C were washed once with distilled water. Purified hydrogels were frozen at -20 °C for a day. Frozen gels were put into the lyophilizer and taken dry from the lyophilizer one day later. The initial weights of the gels taken were weighed. This value is considered as the data for the “t=0 minute” time point. Afterward, they were incubated in distilled water and at room temperature.

Swelling Ratio (%) =

((measured weight of H – the dry weight of H) / dry weight of H) x100 (eq2)

The hydrogels were weighed at certain time intervals (once every 5 minutes). These measurements were continued until the weight of the swollen hydrogel was seen to be stabilized.

4. RESULTS

4.1 Preparation of UV-Curable Hydrogel Scaffolds

4.1.1 Preparation of TEGD-PE hydrogel

Before starting the experiment associated with hydrogel preparation, all the mol equivalent ratios of utilized chemicals (polymers, initiators, and peptides) were calculated and transformed to μL value for their corresponding stock solutions by using an auto-calculation system as shown in the above-mentioned "gel preparation procedure".

Briefly 100.83 μL TEGD was mixed with 24.56 μL PE and DMPA were weighted. Photoinitiator was dissolved in an organic solvent, DMF, and its stock solution with a ratio of 1:4 was prepared. Photo-initiator was added to the mixture in a dark environment from the stock solution and gently sonicated to get prepared for UV curing. Two types of UV sources weak (Analytik Jena UVP BlackRay 6 watt 365 nm) and strong (Analytik Jena UVP BlackRay 100 watt 365nm) were used with both photo-initiators (DMPA & Irg) to optimize the gelation process. DMF was added as an organic solvent to obtain a pre-defined solvent-solute ratio. UV exposure time was set as either 1 hour for strong UV sources or overnight for weak UV sources for both initiators (DMPA and Irg). Obtained gels were freeze-dried overnight and lyophilized gels were stored at -20 °C for further characterization studies.

Table 4.1. Composition details of TEGD-PE hydrogels

No	TEGD (µL)	PE (µL)	DMPA (mg)	Irgacure (mg)	UV (nm/h)
1	100.83	24.56	2.84	-	365/1h
2	100.83	24.56	2.84	-	365/Overnight
3	100.83	24.56	-	2.84	365/1h
4	100.83	24.56	-	2.84	365/Overnight

4.1.2 PLA incorporated hydrogel scaffolds

Briefly, solutions of terminal propargyl ether bearing PLA polymer with 25, 50, and 100 mg were weighted separately in vials and dissolved in 300 µL DMF solvent via sonicator.

Pre-determined amounts of TEGD and PE were added into prepared PLA solutions. Photo-initiator was dissolved in organic solvent DMF and a stock solution with a ratio of 1:4 was prepared. Photo-initiator was added into these mixtures in a dark environment from the stock solution and gently sonicated to get prepared for UV curing. DMF was added as an organic solvent to obtain a pre-defined solvent-solute ratio. The prepared gel solutions were subjected to UV light for 1 hour under a strong UV source. Obtained gels were washed out by first DMF and then distilled water to remove any DMF residual and freeze-dried overnight. Lyophilized hydrogels were stored at-20 °C for further characterization studies.

Table 4.2. Composition details of PLA incorporated hydrogels

No	TEGD (µL)	PE (µL)	Irgacure (mg)	DMF (µL)	PLA %(w/w) / mg
5	100.83	24.56	2.48	130	0
6	100.83	24.1	2.48	149	5% / 25
7	100.83	23.27	2.48	337	10% / 50
8	100.83	20.68	2.48	411	20% / 100

4.1.3 HA encapsulated hybrid hydrogel scaffolds

Briefly, 50 mg of terminal propargyl ether bearing PLA polymer was weighted in a vial and dissolved in 300 µL DMF solvent via sonicator.

Pre-determined amounts of TEGD and PE were added into prepared PLA solutions. Solutions of HA polymer with a pre-defined ratio (21, 42, and 95 mg) were prepared in deionized water. These HA solutions were added onto PLA solutions (in DMF) and mixed gently. A stock solution of photo-initiator was prepared and pre-calculated volumes from this solution were added onto these mixtures separately in a dark environment, sonicated gently to obtain a uniform solution, and prepared for UV curing. Extra DMF and water were added into these mixtures to make the organic: aqueous solvent ratio up for pre-defined solvent-solute ratio.

Gels were subjected to UV light for 1 hour under a strong UV source. Obtained gels were washed out by first DMF and then distilled water to remove any DMF residual and freeze-dried overnight. Lyophilized hydrogels were stored at -20 °C for further characterization studies.

Table 4.3. Composition details of HA encapsulated hybrid hydrogel scaffolds

No	TEGD (µL)	PE (µL)	Irgacure (mg)	PLA %(w/w) / mg	HA %(w/w) / mg	Solvent (DMF+H_2O) /Solute Ratio
9	100.83	23.27	2.48	10% / 50	0	1:4
10	100.83	23.27	2.48	10% / 50	5% / 20	1:4
11	100.83	23.27	2.48	10% / 50	10% / 42	1:4
12	100.83	24.56	2.48	10% / 50	20% / 95	1:4

4.1.4 RGD immobilized (TEGD-PE-PLA+HA) hybrid hydrogels

Briefly, 50 mg of terminal propargyl ether bearing PLA polymer was weighted in a vial and dissolved in 300 µL DMF solvent via sonicator.

Pre-determined amounts of TEGD and PE were added into prepared PLA solutions. Solutions of HA polymer with a pre-defined ratio (42 mg) were prepared in deionized water. These HA solutions were added onto PLA solutions (in DMF) and mixed gently. On the other side, RGDC and IKVAVC peptides were synthesized by the solid-phase peptide synthesis method and purified via the Liquid Phase Chromatography technique. Synthetized peptides were dissolved in DMF separately and added to the prepared gel solutions. A stock solution of photo-initiator was prepared and pre-calculated volumes from this solution were added onto these mixtures separately in a dark environment, sonicated gently to obtain a uniform solution, and prepared for UV curing. Extra DMF and water were added into these mixtures to make the organic: aqueous solvent ratio up for pre-defined solvent-solute ratio.

Gels were subjected to UV light for 1 hour under the strong UV source. Obtained gels were washed out by first DMF and then distilled water to remove any DMF residual and freeze-dried overnight. Lyophilized hydrogels were stored at -20 °C for further characterization studies.

Table 4.4. Composition details of RGD immobilized (TEGD-PE-PLA+HA) hybrid hydrogel scaffolds

No	TEGD (µL)	PE (µL)	Irgacure (mg)	PLA (mg)	HA %(w/w) / mg	RGDC (mg)	IKVAVC (mg)
13	100.8	23.27	2.48	50	42	6.93	-
14	100.8	23.27	2.48	50	42	-	14

4.2 Characterization of Prepared Hydrogel Scaffolds

4.2.1 Gel conversion determination

Gel conversions were calculated according to the procedure mentioned above. Briefly, the glass vials were weighted empty and weighed after the gelation procedure. The rate is calculated according to the equation as a percentage rate.

Gel Conv. = (weight of obtained H / feed weight of H components) x100 (eq. 1)

For each step, gel conversion was calculated for the optimization of the hydrogels.

Table 4.5. Calculated gel conversions of TEGD-PE hydrogel scaffolds

No	Feed weight of gel components (mg)	Weight of Obtained Gel (mg)	Gel conversion %
1	340	220	65.5
2	350	345	70.2
3	377	330	87.6
4	348	293	84.3

Table 4.6. Calculated gel conversion of PLA incorporated hydrogel scaffolds

No	Feed weight of gel components (mg)	Weight of Obtained Gel (mg)	Gel conversion %
5	354	287	87.1
6	393	300	76.5
7	405	347	85.7
8	412	350	84.9

Table 4.7. Calculated gel conversions of (TEGD-PE-PLA+HA) hybrid hydrogel scaffolds

No	Feed weight of gel components (mg)	Weight of Obtained Gel (mg)	Gel conversion %
9	404	333	82.5
10	423	276	65.3
11	430	366	85.2
12	442	346	78.4
13	427	354,8	83.1

Table 4.8. Calculated gel conversions of peptide immobilized (RGD or IKVAV) bioactive hydrogel scaffolds

No	Feed weight of gel components (mg)	Weight of Obtained Gel (mg)	Gel conversion %
13	427	354,8	83.1
14	430	345,6	80.3

4.2.2 Water uptake capacity determination

For the water uptake capacity determination studies, freeze-dried gels were weighted with analytical balance, and gels were thrown into deionized water. During the incubation period at room temperature, swollen hydrogels were weighed using the same analytical

balance. Gels were weighted every 5 minutes and this procedure continued until a stabilization point.

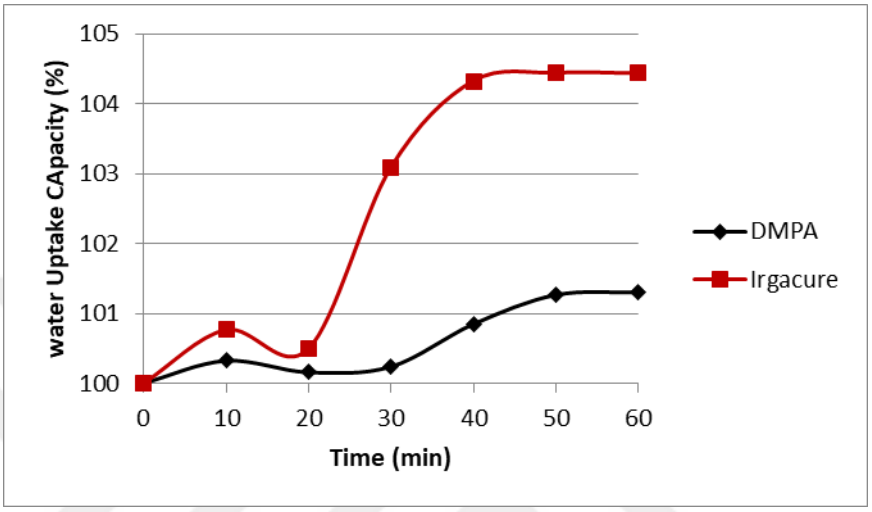

Figure 4.1. Water uptake capacity of UV crosslinked hydrogels

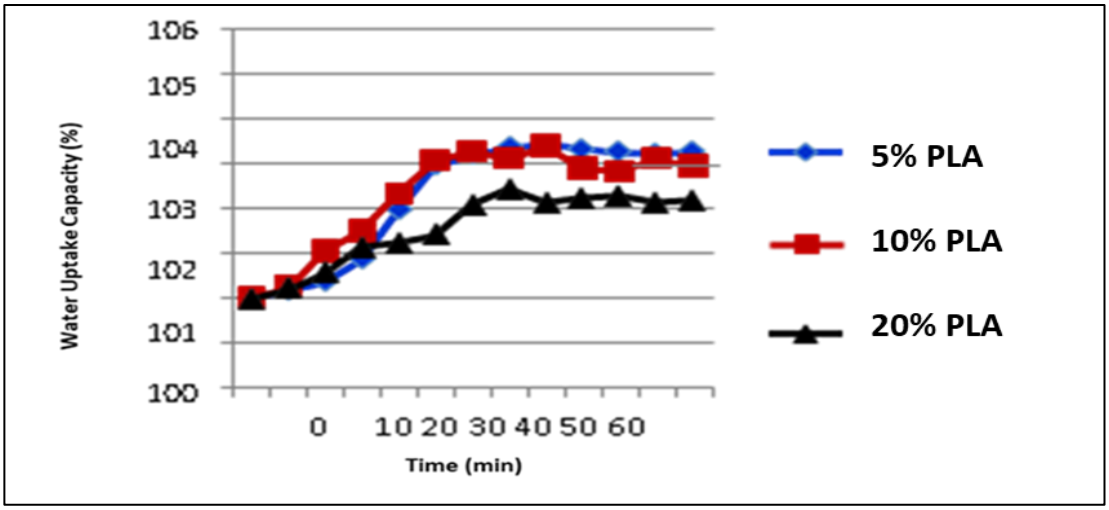

Figure 4.2. Water uptake capacity of PLA incorporated hydrogels

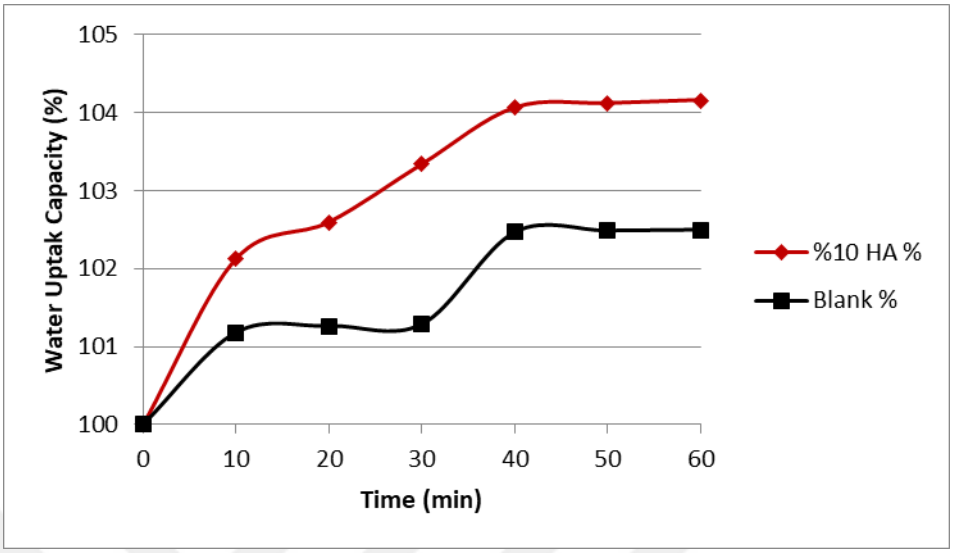

Figure 4.3. Water uptake capacity of HA encapsulated hydrogels

4.2.3 FT-IR spectroscopy Analysis

FT-IR measurements were performed with Thermo Scientific Nicolet iS10 device and the results were analyzed with OMNIC FT-IR Software. This analysis was done to understand the functional groups in prepared hydrogel scaffolds. The chemical diversity of these hydrogels would point into different peaks in obtained FT-IR spectra, which are originated from the functional groups in mainly PLA and HA incorporated into the chemical structure of hydrogels. Each form of designed hydrogels was analyzed by FT-IR in dry form with air as background, and then they were compared with each other and based on their chemical composition.

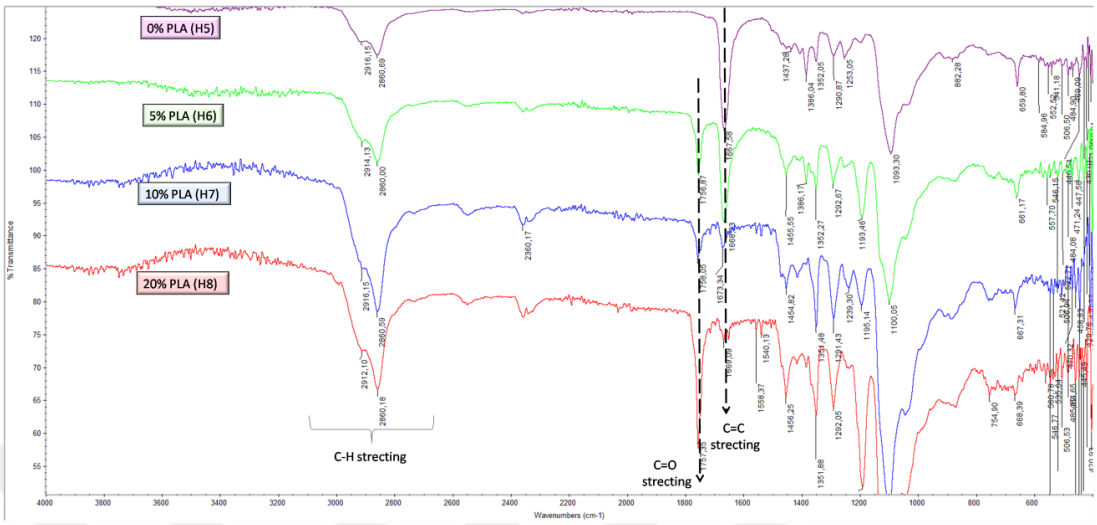

Figure 4.4. FT-IR spectroscopy analysis result for PLA incorporated hydrogels

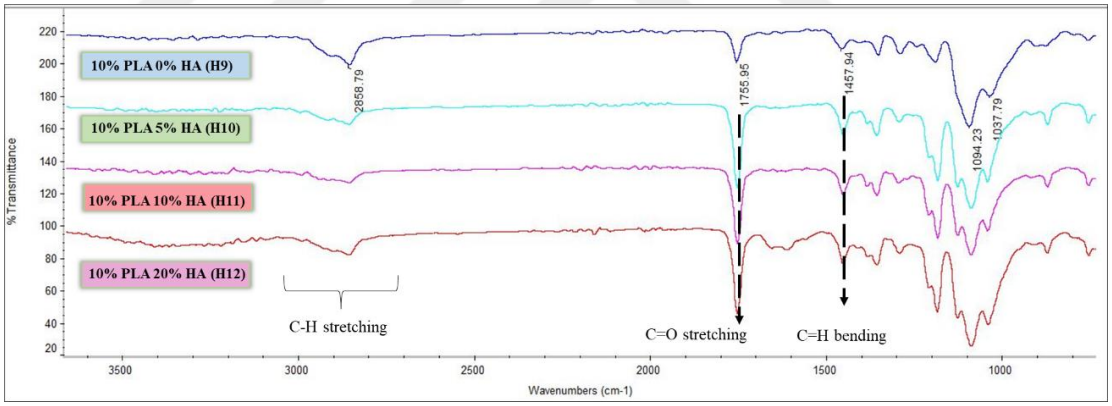

Figure 4.5. FT-IR spectroscopy analysis results of PLA incorporated &HA encapsulated hydrogels

4.2.4 Rheological analysis

Malvern Kinexus ultra+ brand rheometer was used for rheological analysis. The necessary procedure was created at the interface of the device, and the measurements were carried out at 37 °C with a geometry of 40 mm following the procedure. The layer height was 0.02.mm for each sample.

Given the details in the Methods section, each form of designed hydrogels was evaluated by their mechanical properties. Since the incorporation of different amounts of the synthetic polymer PLA was expected to change not only the biodegradation profile of hydrogels but also their stiffness, increased amounts of PLA in hydrogels were analyzed mechanically. Figure 4.6 allows the comparison of mechanical properties of hydrogels with different PLA amounts and highlighted regions represent the same frequency range for better comparison. After encapsulation of long HA polymer chains into hydrogel structures, the remarkable change in deformation profile can be seen in Figure 4.7. Likewise, the impact of increasing amounts of hydrogels with fixed PLA percent on resultant mechanical properties of scaffolds can be evaluated comparably in this Figure.

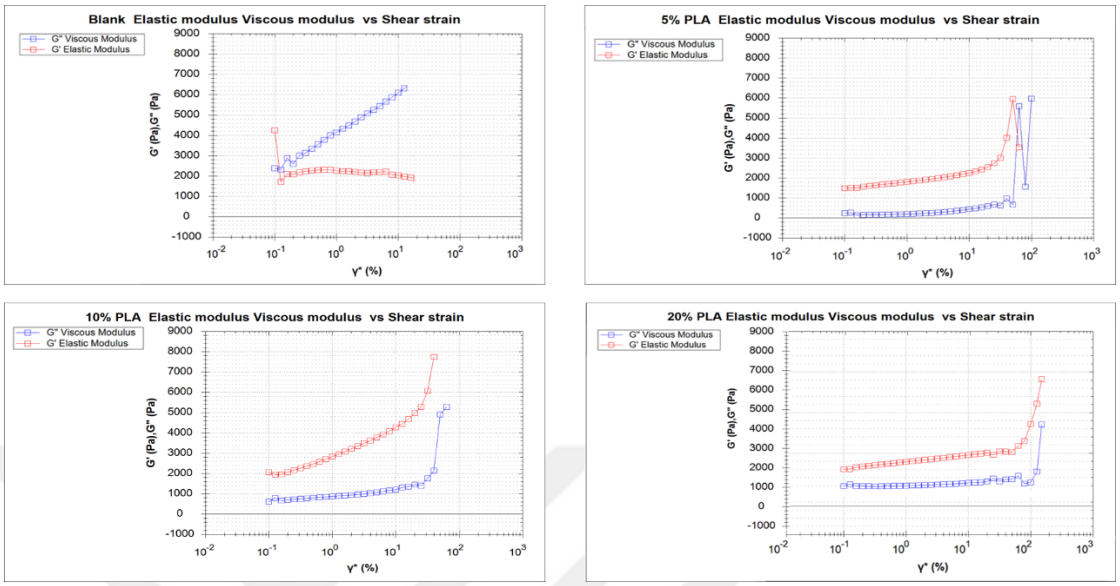

Figure 4.6. Rheological assessments for PLA incorporated gels

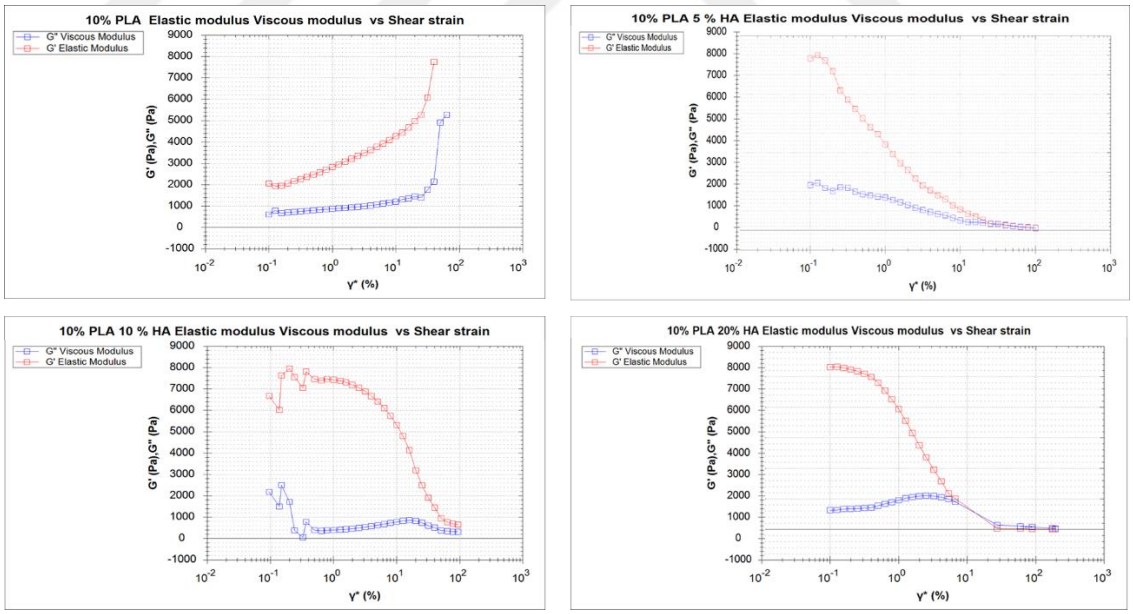

Figure 4.7. Rheological assessments of PLA incorporated &HA encapsulated gels

4.2.5 Morphological analysis

These hydrogel structures, which are expected to have a porous structure, are visualized using Scanning Electron Microscopy (SEM), how porous they are, and their pore sizes.

As subjected to high energy electrons in a high vacuum chamber of SEM instrument, porosity degree, pore sizes, and polymer wall smoothness for different designs of hydrogel scaffolds can be observed in Figures 4.8 and 4.9. SEM images provide information about the morphological change of H1 hydrogel with the attachment of an increasing amount of PLA polymer. On the other hand, Figure 4.9 gives information about the interpenetrated hydrogels obtained by encapsulation of HA chains in the scaffold structures. Similarly, it is possible to compare the obtained SEM images in terms of amounts of HA polymer in the gelated scaffolds.

As an advantage of having an EDS detector in our microscopy facility, it became possible to investigate the prepared bioactive hydrogels in terms of their elemental analysis as atomic and their weight percentages. Figures 4.10 and 4.11 demonstrate the scanning results of the selected area for hydrogels conjugated to RGD and IKVAV adhesion peptides, respectively. Their corresponding atomic and weight percentages obtained by EDS-SEM semi-quantitative analysis are revealed in Tables 4.9 and 4.10 and can be compared with the values obtained for no-peptide conjugated hydrogel at Table 4.8.

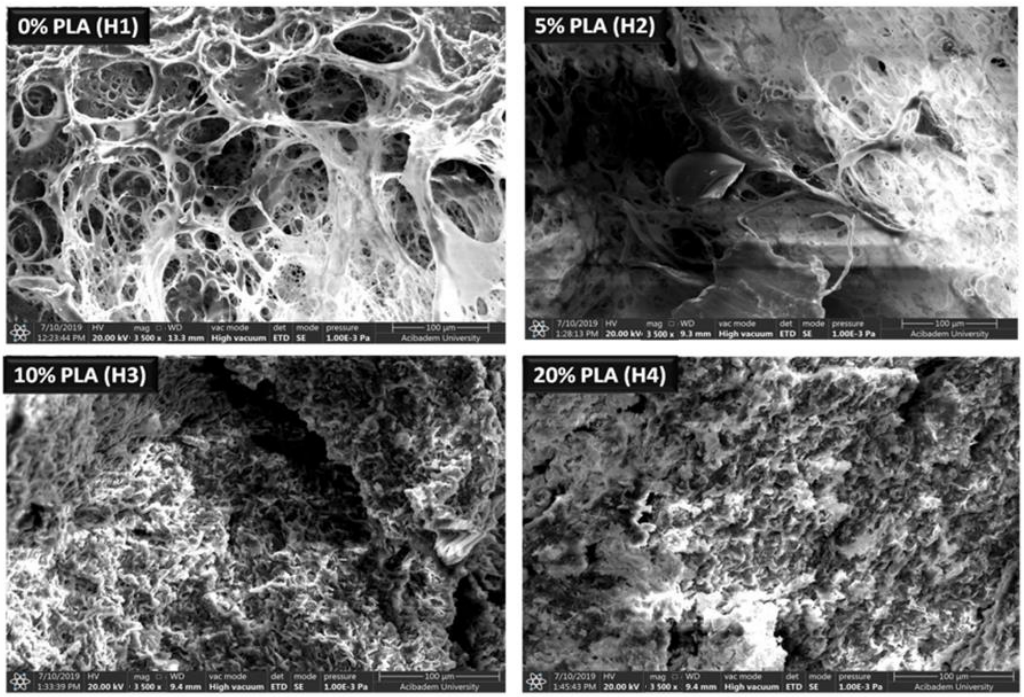

Figure 4.8. Morphological analysis of PLA incorporated gels

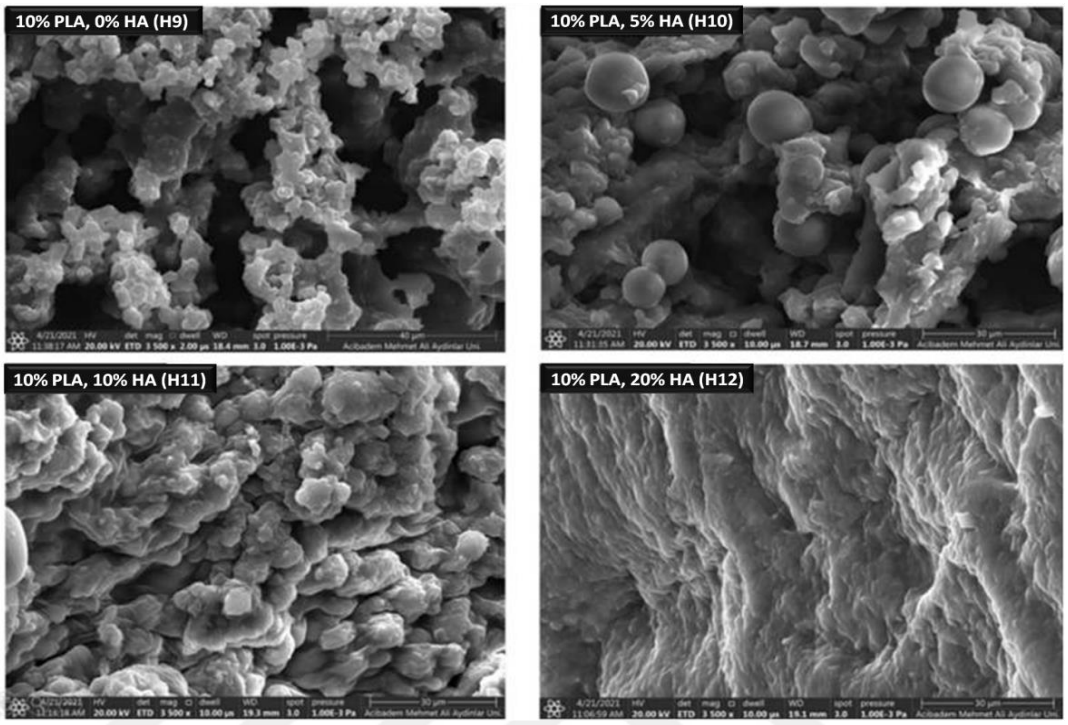

Figure 4.9. Morphological analysis of PLA incorporated &HA encapsulated gels

Table 4.9. Element weight and atomic ratios obtained by SEM-EDS analysis for PLA incorporated & HA encapsulated hydrogel (H11)

Element	Weight %	Atomic %
C	45.14	58.46
N	0	0
O	30.64	29.79
S	24.22	11.75

Table 4.10. Element weight and atomic ratios obtained by SEM-EDS analysis for PLA incorporated & HA encapsulated peptide (RGD) immobilized hydrogel (H13)

Element	Weight %	Atomic %
C	45.08	60.37
N	0.26	0.30
O	23.65	23.77
S	31.01	15.56

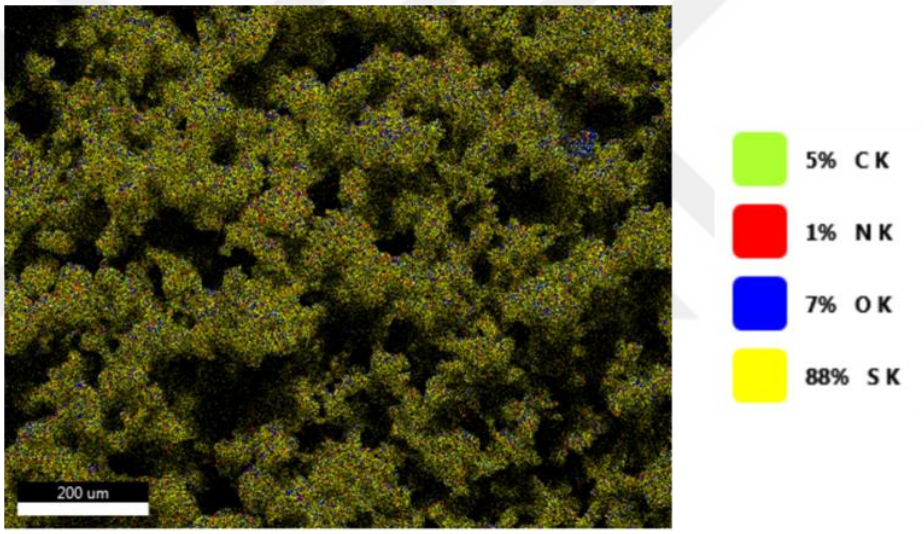

Figure 4.10. EDS-SEM Analysis Result: Scan mode image of PLA incorporated &HA encapsulated peptide (RGD) immobilized hydrogel (H13)

Table 4.11. Element weight and atomic ratios obtained bySEM-EDS analysis for PLA incorporated & HA encapsulated peptide (IKVAV) immobilized hydrogel (H14)

Element	Weight %	Atomic %
C	43.7	58.6
N	0.35	0.25
O	22.8	22.8
S	29.7	14.7

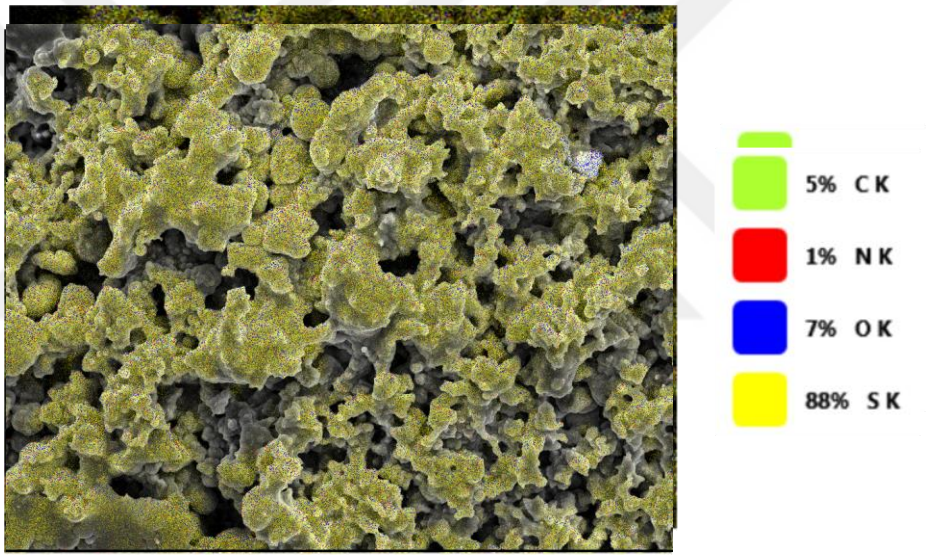

Figure 4.11. EDS-SEM Analysis Result: Scan mode image of PLA incorporated &HA encapsulated peptide (IKVAV) immobilized hydrogel (H14)

4.3 3D Modelling and Printing

Since the hydrogels designed in this study were aimed to be utilized as scaffolds with pre-defined shapes and aligned fiber structure to be advantages in especially neural tissue engineering, their 3D bio-printability was also studied within the context of this thesis. Firstly a thermoreversible synthetic polyester polymer PCL was used to obtain the printable scaffold designs with the 3D Bioprinter present in the laboratory (AxolotlBio dual head, Temp and UV curing). Figure 4.11 represents the designed layouts that are possible to obtain with this bioprinter. The optimization of parameters for the bioprinting process like pressure and speed of head were also evaluated. Later on, these parameters were used as starting point for the bioprinting of the prepared gel mixture developed in this study. The composition of hydrogels with and without PLA and HA was studied in this instrument. Firstly the viscosity of the polymeric mixture was determined to be set to 25% w/v for better printability and to obtain defined shapes of polymeric fibers on a glass slide. Then printed polymeric fiber layers were subjected to UV light for 1 hour with a strong illumination UV source. Figure 4.12 demonstrates the water-washed look of UV cured and 3D printed bioactive hydrogel scaffold, which contains RGD peptide molecules immobilized into its structure.

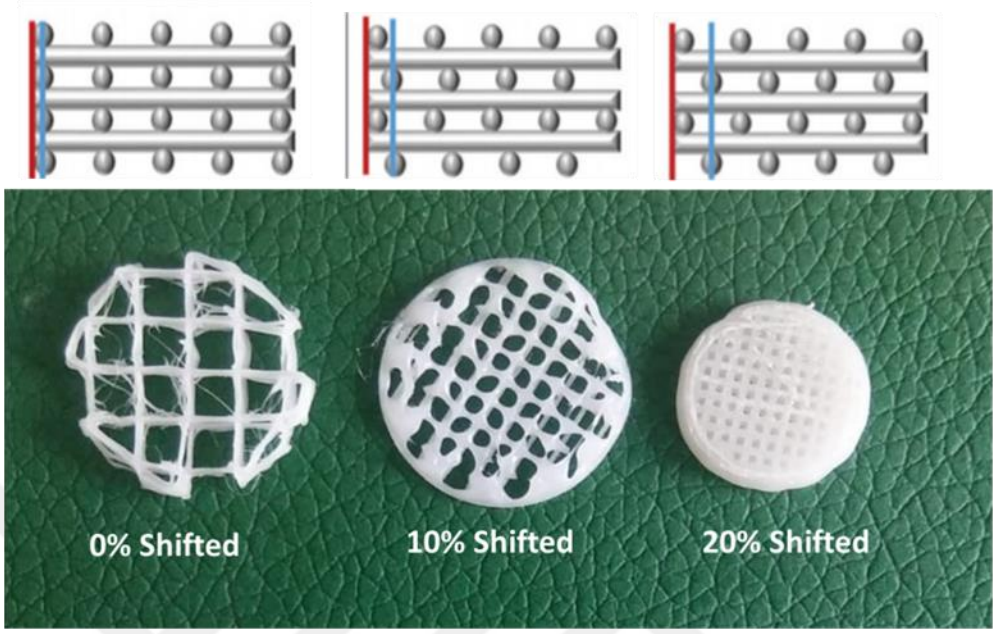

Figure 4.12. 3D Printed PCL (poly-caprolactone) prototypes in different architectures with optimization purposes. (3D printing was conducted with AxoltBio G3 Pneumatic Driven Extrusion. 0.2mm nozzle was used for extrusion with 55 kPa and 205 C° The printing speed gor first layer was 60 mm/s and the layer 0.2mm.)

Figure 4.13. Photo for 3D Printed bioactive hydrogel scaffold obtained in this thesis. (3D printing was conducted with AxoltBio G3 Pneumatic Driven Extrusion. 18G gauge was used for extrusion with 70 kPa and 36C° The printing speed gor first layer was 30 mm/s and the layer 0.2mm.Repetier Host slicer was used for shape and size adjustments.)

5. DISCUSSION

Hydrogels prepared in this thesis were designed as suitable scaffolds for nerve cell adhesion which is expected to help attachment and migration of surrounding healthy neurons in an injured area. The aim here is to provide damaged tissues with neural connection restore, hopefully, followed by improved communication of nerve cells for electrical signal conduction for neural tissue regeneration as an effective therapy for diseases related to nerve damage like spinal cord injury and acute peripheral ischemia. (22)

So, both synthetic and natural polymeric biomaterials were utilized to prepare the scaffolds in this study, and then they were decorated with either a general cell adhesion peptide RGD or a nerve-cell specific one IKVAV. To benefit from the adhesion impact of these peptides on cells, they were functionalized with a free thiol group to participate in the gelation reaction so that they were immobilized into the resultant hydrogel structure until it is degraded under physiological conditions. (19)

Engineering the features of hydrogel scaffolds to be more convenient for neural cell adhesion started with designing the architecture which was successfully obtained as porous yet well-defined by thiol-yne chemistry. Unlikely the literature, in this study radical addition of thiol groups on tetra (ethylene glycol) dithiol to terminal alkyne groups of propargyl ether were conducted by UV-assisted Thiol-yne reaction for eliminating the presence of leftover thiol groups and double bonds in hydrogel structure, which would be safer for biological experiments with cells in *in vitro* and *in vivo* applications by removing the possibility of any side reaction with the active compounds in a biological environment. (10)

The prepared gels were obtained by optimizing lots of parameters like the type of radical source as photo-initiators, the strength of UV light source, gelation time, and solvent-solute ratio. Based on the obtained gel conversion results, Irg with a %87.6 value was selected to go further in hydrogel design. As seen in Table 4.5, it was gelated under a strong UV light source for 1 hour, which gave gel structures in a shorter period (1h) with the highest gel conversion.

Since mechanical properties of scaffolds for neural tissue engineering is very important for both neuron attachment and differentiation, these UV-curable gels were incorporated with a synthetic polymer PLA, which is known well for its assertive impact on improving mechanical properties. (23) 3 different amounts of PLA were utilized to participate in the thiol-yne reaction for gelation from the terminal alkyne units at one end of its chain. Obtained gels were also investigated for their gel conversions to be more than %80. Among the obtained gels, with PLA whose water-holding capacities are shown in Figure 4.2. Comparatively, it is observed that the gel containing 10% PLA polymer exhibits a more similar profile to the pure gel formulation. Since the gel containing 5% PLA disintegrated after the first few weighings, the water retention profile graph could not be obtained stably. It is thought that the reason why the gel containing 20% PLA polymer showed lower water holding capacity most probably due to the hydrophobic chemical structure of the PLA polymer.

For the characteristic peaks of the gels whose FT-IR spectra are given comparatively in Figure 4.4, it is seen that the peaks of the carbonyl bonds (~1750 cm^{-1}) from the chemical structure of PLA, which is a polyester polymer, compared to the blank gel can be seen as newly emerged peaks. In addition, it is seen that the amount of free and unreacted double bonds (~1670 cm^{-1}) that is released after the gelation reaction decreases with the increase in the PLA percentage in the environment.

Based on especially mechanical properties of PLA-incorporated gels, it is obvious that the G' representing the solid phase as storage modulus gets higher by the increasing amount of PLA in the gel structure. In all graphs given comparatively in Figure 4.6 and Figure 4.7, for the rheological analyses, the blue curve is considered as the G'' value and indicates the elastic (liquid) phase. The red curve is the G value and indicates the viscous (gel) phase. Therefore, it is observed that the G' value is greater than the G'' value for all hydrogels, indicating that all hydrogels obtained are durable and stable. In addition, it can be observed in all results that the red curves of all hydrogels that indicate the solid phase cannot fully maintain their stability when a high-frequency shear force is applied, but they are still larger than the blue curves of the liquid phase. By looking at the gap between the G' and G'' curves, it can be seen that the solid phase of the hydrogel containing 10% PLA is much more stable than the liquid phase. On the other side, 20% PLA containing hydrogel seems not to provide a well-observed porous structure. So 10% PLA content was determined to be optimum to continue with for further hydrogel design.

In the images taken under high vacuum and with the EDS detector, it is seen that in Figure 4.8 the hydrogel which does not contain any PLA polymer, has a highly porous structure. On the other hand, it was observed that the hydrogel containing 5% PLA had irregularities in its morphology and the pores were not very prominent. When PLA polymer is added to the hydrogel consisting of ethylene glycol structures, the possibility that a low PLA ratio in the gel may cause hydrophilic/hydrophobic phase separation is also encountered in the literature. (24) In this study, it was thought that the possibility of this phase separation may be the cause of the instability of the hydrogel containing 5% PLA and its structure that disintegrates in a short time (max 15-20 minutes) in water. Hydrogels containing 10% and 20% PLA have similar morphology and similar porosity density and size from the images taken at the same magnification.

Since the ethylene glycol chain in the obtained gel structure is so short to provide a soft tissue model, it was needed to include a hydrophilic polymer inside. The literature points out that specifically, the hyaluronic acid polymer is a very well-suited biomaterial that is widely used for fabrication scaffolds for neural tissue engineering. (25) Both adhesions of nerve cells and their migration profile seem to be better with these polymeric well-associated scaffolds. In the light of this information, the gels optimized here were also added with different amounts of HA polymer, which required to use of water as a co-solvent for the gelation process. Since it is miscible with DMF used to dissolve other components of designed gels, no precipitation was observed during the preparation of the gel mixture.

The presence of HA chains in obtained gel scaffolds after washing steps was confirmed by FT-IR analysis by looking at the increased intensity of broad peaks at ~3300 cm^{-1} and also the peak representing –C-O- bonds at ~1050 cm^{-1} coming from HA structure mainly and entrapped HA chains in the formulation was found to provide better swelling ability, which supports hydrogel characteristic of the resultant gel. As seen in Figure 4.3 the results show that the hydrogels containing hyaluronic acid prepared in the next steps can swell to a greater extent and faster than the main scaffold structure, in the water holding capacity experiment. It can also be concluded that the hydrogel containing 10% HA swells more than the gel, which is called the main structure, and retains this water for a long time. The water retention graph could not be obtained stably for both gels that contain 20% and 5% HA since the hydrogels were disintegrated may be due to the hydrophilic nature of HA.

In the SEM images taken under a high vacuum (Figure 4.9), it was observed that there are irregularities in the morphology of the hydrogel containing 5% HA and the pores are not very prominent. The possibility that the HA molecule can cause hydrophilic/hydrophobic phase separation when added to the hydrogel consisting of PLA

polymer and ethylene glycol structures is also encountered in the literature. (26) In this study, it was thought that the possibility of this phase separation may be the reason for the instability of the hydrogel containing 5% HA and the control hydrogel. Both the entrapped HA polymer chains and PLA polymer chains can be seen to contribute to polymeric walls of the obtained scaffold in the images taken at the same magnification as that of the hydrogel containing 10% HA. So it is understood from the image taken that the hydrogel containing 10% HA has a porous structure and the pore size varies mostly between 4-9 μm at 3500X.

A proper deformation profile was reached for hydrogels with the entrapment of HA chains inside, which was revealed by rheological analysis. In Figure 4.7, all rheological experiments for HA containing hydrogels seem to reveal a deformation after a certain pressure application compared to hydrogel without HA in its structure. The cross-point of G' and G'' curves represent the switch of hydrogel's stiffness from solid-like to liquid-like phase. Notably, entrapment of HA chains in the structure improves this trend, which is very significant in terms of biodegradability and elasticity of the resultant scaffold. It is expected for this kind of 3D scaffold to adapt to its environment shape-wise based on the applied pressure. So with this experiment, it is proved that the obtained HA containing hydrogels become softer and mechanically more responsive. Although this deformation profile is more obvious for hydrogel with 20% HA, its gel conversion was relatively lower and pores were observed as smaller. That is why out of 3 different formulations containing varying HA amounts, 10% HA containing hydrogel was selected to be more suitable for peptide immobilization to make this 3D network more biomimetic and bioactive.

To obtain peptide-linked hydrogels, RGD peptide (RGDC) containing the free thiol group was added to the medium during the gelation reaction. The hydrogel containing 10% PLA and %10 HA, was selected as the hydrogel composition with the most suitable

properties after the characterization steps specified was prepared with the same proportions of all materials concerning each other, but 0.5% (moles) of the free thiol group in the medium was RGDC peptide. The quantities of materials used are clearly shown in Table 3. The obtained peptide hydrogel was also purified by washing 2 times with pure DMF and then 2 times with distilled water, lyophilized by freezing, and stored at +4 °C in dry form.

By using the EDS detector integrated into the SEM microscope, both the morphological imaging of the peptide-linked hydrogel and the atoms in its structure could be examined semi-quantitatively. The peptide-bound hydrogel was prepared using the sample preparation procedure described and visualized using the ESEM detector under a low vacuum, maximally swollen with water. It can be seen from the image taken that the peptide bonded hydrogel has a porous structure and the pore size is 3500X, mostly between 3-6 μm.

As a result of the atom diversity and quantification by sending X-rays with the EDS detector, peaks belonging to the Nitrogen (N) atom were observed in the spectrum of the peptide bond. This extra N peak compared to the hydrogel without peptide indicates the presence of peptide molecules integrated and fixed in the structure of the hydrogel. After a semi-quantitative comparison of the atomic peaks in the spectra obtained from the hydrogels, it was concluded that the structure of the hydrogel was 0.11% by mass, and approximately 10% of the peptide that was initially introduced into the thiol-yne reaction was incorporated into the hydrogel structure.

6. CONCLUSION

The aim of this project is the preparation of a biomaterial platform that can be used as the main scaffold material in diseases associated with nerve tissue damage and within the experiments conducted in this thesis, different hydrogel scaffolds have been accomplished to be prepared successfully and characterized from lots of aspects. The data obtained and the experience gained in this project will lead to the preparation of more specific and tailor-made soft artificial tissue pieces that can be an effective part of therapies used for the recovery of nerve cell functioning in especially peripheral neural tissue associated damage based diseases.

According to the results obtained after all the characterization steps, since its water holding capacity is similar to the ethylene glycol-based (gel with 0% PLA) hydrogel in terms of its stable structure and the rheological durability of the gel phase, it did not react less than other hydrogels after gelation in the functional group analysis. Since it contains double bonds and considering the smoothness of the porosity structure, it was decided that the hydrogel containing 10% PLA has optimum properties, and hydrogels were prepared using these ratios to obtain peptide-conjugated hydrogels, which is the next step of the project. Based on the FT-IR spectra and gel conversion efficiency data of the prepared gels, it was proven that the “Irgacure” photoinitiator provides more efficient gelation under UV, and the experiments were continued in the light of this information. After the specified characterization steps, the hydrogel containing 10% PLA and 10% HA was selected as the hydrogel composition with the most suitable properties and then was utilized for the preparation of bioactive hydrogel scaffolds by peptide conjugation.

The quantities of materials used are clearly shown in Table 5. These 3-dimensional scaffolds (scaffolds), in which the RGD-C peptide, which improves cell adhesion in

general, is immobilized with covalent bonds into scaffold structure. Also, a more specific peptide for nerve cells, IKVAV, was used for this kind of conjugation and IKVAV-immobilized hydrogels were also prepared successfully.

On the other hand, the mechanical properties of hydrogels were adjusted wisely to adapt them specifically to the natural human neural tissue. For this, both the durability and flexibility of the scaffold were made to increase with PLA and HA polymers, together with the improving contribution to water holding capacity. Moreover, these cross-linked hydrogels, which are expected to have a slow degradation rate under physiological conditions at neutral pH value, tend to deform at high pressure, which strengths its potential for biomedical use to provide a long-term therapeutic effect.

7. REFERENCES

1. Spicer CD. Hydrogel scaffolds for tissue engineering: The importance of polymer choice. Polym Chem [Internet]. 2020;11(2):184–219. Available from: http://dx.doi.org/10.1039/c9py01021a

2. Catoira MC, Fusaro L, Di Francesco D, Ramella M, Boccafoschi F. Overview of natural hydrogels for regenerative medicine applications. J Mater Sci Mater Med [Internet]. 2019;30(10). Available from: http://dx.doi.org/10.1007/s10856-019-6318-7

3. Nezhad-Mokhtari P, Ghorbani M, Roshangar L, Soleimani Rad J. A review on the construction of hydrogel scaffolds by various chemically techniques for tissue engineering. Eur Polym J. 2019;117(April):64–76.

4. Unal AZ, West JL. Synthetic ECM: Bioactive Synthetic Hydrogels for 3D Tissue Engineering. Bioconjug Chem. 2020;31(10):2253–71.

5. Macdougall LJ, Pérez-madrigal MM, Arno MC, Dove AP. cytocompatible soft tissue scaffolds Contents. :1–17.

6. Perrier B. Dendritic Polymers from Thiol – Yne Reactions. 2009;(6).

7. Konkolewicz D, Poon CK, Gray-Weale A, Perrier S. Hyperbranched alternating block copolymers using thiol–yne chemistry: Materials with tuneable properties. Chem Commun. 2011;47(1):239–41.

8. Prasath RA, Gokmen MT, Espeel P, Du Prez FE. Thiol-ene and thiol-yne chemistry in microfluidics: A straightforward method towards macroporous and nonporous functional polymer beads. Polym Chem. 2010;1(5):685–92.

9. Tam RY, Cooke MJ, Shoichet MS. A covalently modified hydrogel blend of hyaluronan-methyl cellulose with peptides and growth factors influences neural stem/progenitor cell fate. J Mater Chem. 2012;22(37):19402–11.

10. Jennings AR, Son DY. CHAPTER 6. Thiol-ene/yne Chemistry for the Synthesis of Branched and Star-shaped Macromolecules. 2013. 117–150 p.

11. Xu Y, Xu H, Jiang X, Yin J. Versatile functionalization of the micropatterned hydrogel of hyperbranched poly(ether amine) based on “thiol-yne” chemistry. Adv Funct Mater. 2014;24(12):1679–86.

12. Lutz JF, Börner HG. Modern trends in polymer bioconjugates design. Prog Polym Sci. 2008;33(1):1–39.

13. Palmese LL, Thapa RK, Sullivan MO, Kiick KL. Hybrid hydrogels for biomedical applications. Curr Opin Chem Eng. 2019;24:143–57.

14. Gyles DA, Castro LD, Silva JOC, Ribeiro-Costa RM. A review of the designs and prominent biomedical advances of natural and synthetic hydrogel formulations. Eur Polym J. 2017;88:373–92.

15. Mann BK, Tsai AT, Scott-Burden T, West JL. Surface modification with cell adhesion peptides alters extracellular matrix deposition. Annu Int Conf IEEE Eng Med Biol - Proc. 1999;1:94.

16. Auernheimer J, Dahmen C, Hersel U, Bausch A, Kessler H. Photoswitched cell adhesion on surfaces with RGD peptides. J Am Chem Soc. 2005;127(46):16107–10.

17. Schmedlen RH, Masters KS, West JL. Photocrosslinkable polyvinyl alcohol hydrogels that can be modified with cell adhesion peptides for use in tissue engineering. Biomaterials. 2002;23(22):4325–32.

18. Gelain F, Bottai D, Vescovi A, Zhang S. Designer self-assembling peptide nanofiber scaffolds for adult mouse neural stem cell 3-dimensional cultures. PLoS One. 2006;1(1).

19. Sun Y, Li W, Wu X, Zhang N, Zhang Y, Ouyang S, et al. Functional Self-Assembling Peptide Nanofiber Hydrogels Designed for Nerve Degeneration. ACS Appl Mater Interfaces. 2016;8(3):2348–59.

20. Wang S, Sarwat M, Wang P, Surrao DC, Harkin DG, St John JA, et al. Hydrogels with Cell Adhesion Peptide-Decorated Channel Walls for Cell Guidance. Macromol Rapid Commun. 2020;41(15).

21. Waheed S, Cabot JM, Macdonald NP, Lewis T, Guijt RM, Paull B, et al. 3D printed microfluidic devices: Enablers and barriers. Lab Chip. 2016;16(11):1993–2013.

22. Koss KM, Unsworth LD. Neural tissue engineering: Bioresponsive nanoscaffolds using engineered self-assembling peptides. Acta Biomater [Internet]. 2016;44:2–15. Available from: http://dx.doi.org/10.1016/j.actbio.2016.08.026

23. Basu A, Kunduru KR, Doppalapudi S, Domb AJ, Khan W. Poly(lactic acid) based hydrogels. Adv Drug Deliv Rev [Internet]. 2016;107:192–205. Available from: http://dx.doi.org/10.1016/j.addr.2016.07.004

24. Hu X, Tan H, Wang X, Chen P. Surface functionalization of hydrogel by thiol-yne click chemistry for drug delivery. Colloids Surfaces A Physicochem Eng Asp. 2016;489:297–304.

25. Tarus D, Hamard L, Caraguel F, Wion D, Szarpak-Jankowska A, Van Der Sanden B, et al. Design of Hyaluronic Acid Hydrogels to Promote Neurite Outgrowth in Three Dimensions. ACS Appl Mater Interfaces. 2016;8(38):25051–9.

26. Ma H, Caldwell AS, Azagarsamy MA, Gonzalez Rodriguez A, Anseth KS. Bioorthogonal click chemistries enable simultaneous spatial patterning of multiple proteins to probe synergistic protein effects on fibroblast function. Biomaterials [Internet]. 2020;255:120205. Available from: https://doi.org/10.1016/j.biomaterials.2020.120205

27. Northrop BH, Co RN. Thiol−Ene Click Chemistry Computational and Kinetic Analysis of.pdf. J Am Chem Soc. 2012;(134):13804–17.

28. Wang S, Lee JM, Yeong WY. Smart hydrogels for 3D bioprinting. Int J Bioprinting. 2015;1(1):3–14.

29. Hu W, Wang Z, Xiao Y, Zhang S, Wang J. Advances in crosslinking strategies of biomedical hydrogels. Biomater Sci. 2019;7(3):843–55.

8. APPENDICES

Point Inde	Sample De	Action Nai	Time (seq	Time (acti	Temperati	Frequency	Complex s	Complex s	Shear mo	Shear mo	Shear mo	Shear visc	Phase ang	Normal fo	First norm	Gap(mm)	Torque(N	Absolute	Harmonic	Point Note
1	blank sh	Oscillation	30,41	30	36,99	0,1	1,81686	88,59	4,88E+03	2,39E+03	4,25E+03	7,76E+03	60,68	1,552		0,7	1,86E-04	5,932	50	
2	blank sh	Oscillation	58,35	57,95	37,02	0,1259	6,32149	182,6	2,89E+03	2,32E+03	1,72E+03	3,65E+03	36,53	1,513		0,7	3,82E-04	5,944	1,824	
3	blank sh	Oscillation	84,68	84,27	37,01	0,1585	4,45944	159,2	3,57E+03	2,89E+03	2,10E+03	3,58E+03	35,96	1,484		0,7	3,33E-04	5,941	1,13	
4	blank sh	Oscillation	109,7	109,3	37,01	0,1995	5,5674	185,4	3,33E+03	2,60E+03	2,08E+03	2,66E+03	38,7	1,458		0,7	3,88E-04	5,942	0,5524	
5	blank sh	Oscillation	137,7	137,3	37,01	0,2512	4,96195	184,4	3,72E+03	3,01E+03	2,19E+03	2,36E+03	36,04	1,432		0,7	3,86E-04	5,942	0,2127	
6	blank sh	Oscillation	164	163,6	37	0,3162	5,0249	193,8	3,86E+03	3,15E+03	2,23E+03	1,94E+03	35,34	1,409		0,7	4,06E-04	5,935	0,416	
7	blank sh	Oscillation	189	188,6	37,01	0,3981	5,00908	202,7	4,05E+03	3,35E+03	2,27E+03	1,62E+03	34,14	1,387		0,7	4,25E-04	5,937	0,4235	
8	blank sh	Oscillation	215	214,6	37,01	0,5012	4,99372	211,6	4,24E+03	3,56E+03	2,30E+03	1,35E+03	32,84	1,366		0,7	4,43E-04	5,938	0,1764	
9	blank sh	Oscillation	241,4	241	37	0,631	5,00075	221,9	4,44E+03	3,79E+03	2,31E+03	1,12E+03	31,43	1,351		0,7	4,65E-04	5,94	0,2079	
10	blank sh	Oscillation	266,5	266	37	0,7943	5,00593	231,4	4,62E+03	4,00E+03	2,31E+03	926,2	30	1,331		0,7	4,85E-04	5,935	0,1739	
11	blank sh	Oscillation	292,5	292,1	37,01	1	4,99886	236,2	4,73E+03	4,15E+03	2,27E+03	752,2	28,66	1,313		0,7	4,95E-04	5,934	0,1929	
12	blank sh	Oscillation	318	317,6	37	1,259	5,00889	244,2	4,88E+03	4,33E+03	2,25E+03	616,3	27,42	1,298		0,7	5,11E-04	5,935	0,2182	
13	blank sh	Oscillation	343,1	342,7	37	1,585	5,00787	251,2	5,02E+03	4,49E+03	2,24E+03	503,7	26,48	1,283		0,7	5,26E-04	5,938	0,2726	
14	blank sh	Oscillation	368,1	367,7	37	1,995	5,01231	259,5	5,18E+03	4,68E+03	2,21E+03	413	25,32	1,272		0,7	5,44E-04	5,942	0,3326	
15	blank sh	Oscillation	393,3	392,9	37	2,512	5,00639	267,9	5,35E+03	4,89E+03	2,18E+03	339,1	24,06	1,257		0,7	5,61E-04	5,942	0,3792	
16	blank sh	Oscillation	418,4	418	37,01	3,162	5,01804	276,8	5,52E+03	5,08E+03	2,15E+03	277,6	22,92	1,243		0,7	5,80E-04	5,942	0,4803	
17	blank sh	Oscillation	443,5	443,1	37	3,981	5,03414	286,7	5,69E+03	5,25E+03	2,20E+03	227,6	22,69	1,229		0,7	6,00E-04	5,934	0,6406	
18	blank sh	Oscillation	468,7	468,3	37	5,012	5,00453	293,5	5,86E+03	5,44E+03	2,20E+03	186,2	22,04	1,217		0,7	6,15E-04	5,938	0,7432	
19	blank sh	Oscillation	493,8	493,4	37	6,31	5,03312	306,2	6,08E+03	5,66E+03	2,22E+03	153,5	21,44	1,203		0,7	6,41E-04	5,942	1,407	
20	blank sh	Oscillation	518,8	518,4	37	7,943	5,02839	313,4	6,23E+03	5,88E+03	2,07E+03	124,9	19,42	1,192		0,7	6,56E-04	5,941	0,5533	
21	blank sh	Oscillation	543,9	543,5	37	10	4,99594	321,5	6,44E+03	6,10E+03	2,04E+03	102,4	18,51	1,179		0,7	6,73E-04	5,936	0,2111	
22	blank sh	Oscillation	568,9	568,5	37,01	12,59	5,12863	339,3	6,62E+03	6,31E+03	1,98E+03	83,64	17,44	1,169		0,7	7,11E-04	5,942	0,1093	
23	blank sh	Oscillation	594	593,6	37,02	15,85	5,0562	348,9	6,90E+03	6,63E+03	1,93E+03	69,3	16,27	1,157		0,7	7,31E-04	5,936	0,04629	
24	blank sh	Oscillation	619	618,6	37,01	19,95	5,02274	362,5	7,22E+03	6,97E+03	1,88E+03	57,57	15,11	1,146		0,7	7,59E-04	5,942	0,03022	

Figure 8.1. Raw Data for Rhelogical Analyses

Blank		10%		20%	
0	3197	0	1794	0	1918
5	3203	5	1799	5	1922
10	3209	10	1813	10	1929
15	3225	15	1821	15	1940
20	3260	20	1836	20	1942
25	3292	25	1849	25	1945
30	3300	30	1853	30	1958
35	3305	35	1850	35	1965
40	3307	40	1855	40	1959
45	3304	45	1846	45	1961
50	3302	50	1845	50	1962
55	3301	55	1850	55	1959
60	3302	60	1847	60	1960

Figure 8.2. Water Uptake Capacity (Raw Data)

9. CURRICULUM VITAE

Personal Information

Name		**Surname**	
Place of Birth		**Date of Birth**	
Nationality		**Telephone Number**	
E-mail			

Education

	Institution Name	**Graduation Year**
Master of Science		
Undergraduate		
High School		

Work Experience

Position	Corporation	Duration

Foreign Language

Language	Reading*	Speaking*	Writing*

***** Evaluated as advanced, good, intermediate, beginner

Foreign Language Exam Results[#]

KPDS	ÜDS	IELTS	TOEFL IBT	TOEFL PBT	TOEFL CBT	DİĞER

KPDS: Kamu Personeli Yabancı Dil Sınavı; ÜDS: Üniversitelerarası Kurul Yabancı Dil Sınavı; IELTS: International English Language Testing System; TOEFL IBT: Test of English as a Foreign Language-Internet-Based Test TOEFL PBT: Test of English as a Foreign Language-Paper-Based Test; TOEFL CBT: Test of English as a Foreign Language-Computer- Based Test; FCE: First Certificate in English; CAE: Certificate in Advanced English; CPE: Certificate of Proficiency in English

Other Exams

Name of the Exam	Quantitative	Equally Weighted	Verba

****** ALES: Akademik Personel ve Lisansüstü Eğitimi Giriş Sınavı

Computer Skills

Program	Ability to Use